 SNC • LAVALIN	TECHNICAL NOTE Hydrogeological modelling for in-pit tailings deposition		Prepared by: E. Millet, G. Comeau Reviewed by: C.Belanger, H.Sangam	
	SNC No. 651196-3000-4WER-0001 AEM No. 6118-E-132-001-TCR-003	Rev.	Date	Page
		A00	August 16 th , 2018	23

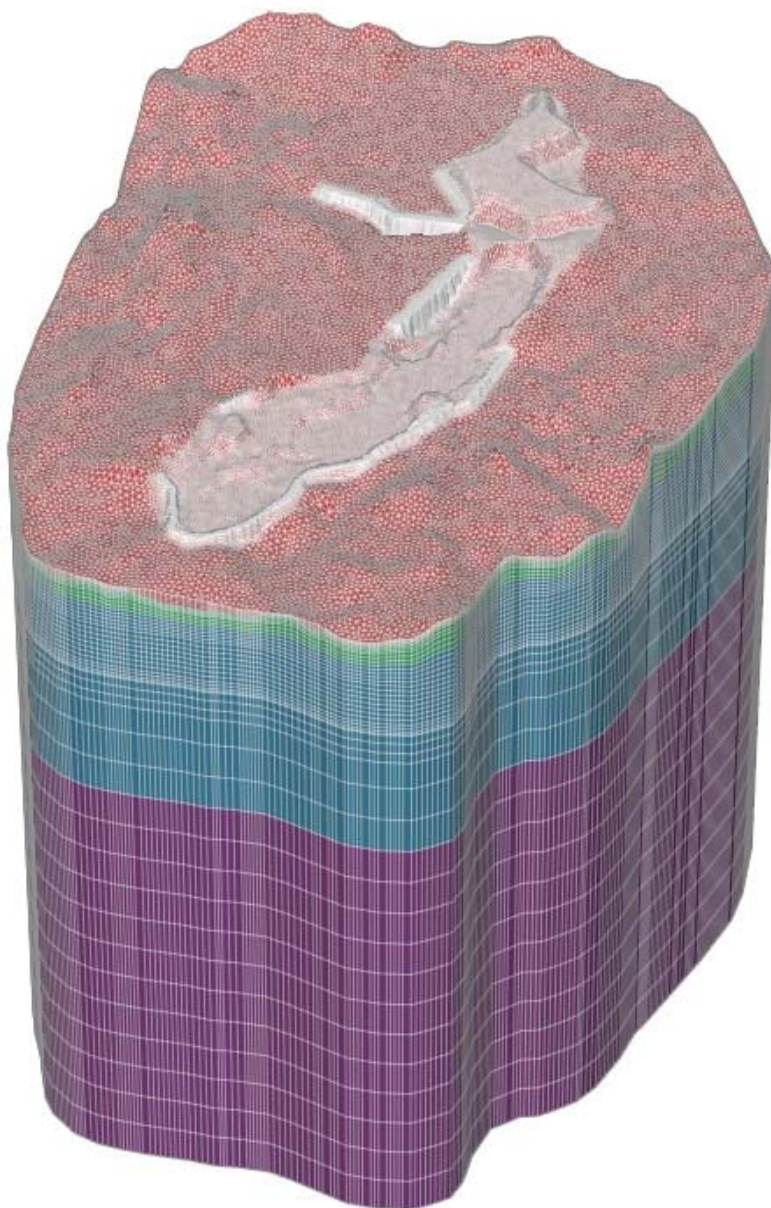



Figure 12 : 3D View of the hydrogeological model

 SNC • LAVALIN	TECHNICAL NOTE		Prepared by: E. Millet, G. Comeau Reviewed by: C. Belanger, H. Sangam		
	Hydrogeological modelling for in-pit tailings deposition		Rev.	Date	Page
	SNC No. 651196-3000-4WER-0001 AEM No. 6118-E-132-001-TCR-003		A00	August 16 th , 2018	24

Model limits


Three types of boundary conditions were used in the model: specified constant heads or fixed heads (where the hydraulic head is kept constant at a given value throughout the flow simulation), drain conditions (seepage face), and no-flow zones (where no flow across the boundary).

Specified constant heads were used as boundary conditions in areas where the model domain is bounded by lakes. These boundary conditions are shown in Figure 13, which also shows the boundary conditions used in the TSF areas as well as the pit areas. The following summarizes the boundary conditions used in the model during pits dewatering operations for calibration purpose:

- > A fixed head of elevation 135 m was applied as the boundary condition for the northwest area. This value was estimated using the regional gradient and the main lake elevation on the north area of Portage Pit E. This fixed head is also applied for the southeast boundary of the model for the Second Portage lake border to allow natural outflow from the model;
- > Fixed heads at the boundary of the model were used on nodes representing Second Portage Lake and Third Portage Lake water elevations (132.9 and 133.6 masl, respectively).
- > Fixed heads were also used to represent North Cell and South Cell with heads of 148.0 and 130.0 masl, respectively. These water elevations were measured in 2016.
- > A drain condition was used for Goose Pit, Portage Pit A, Portage Pit E and Central Dike downstream (D/S) pond to represent the maintained water elevation during pumping;
- > Drain conditions were also set for each pit shell with the available pit wall geometries to represent the 2016 bottom depth of Goose Pit (-11 masl, with a rise of water level up to 41 masl), Portage Pit A (46 masl) and Portage Pit E (4 masl);
- > The two East Dike pumping wells (Figure 13) and observed rates were considered;
- > A no-flow condition was used to represent the impermeable base of the model and also the northeastern border, along a flow line.
- > Zero recharge was assigned on the top of the model since recharge only occurs at open talik locations where hydraulic heads were fixed in the model, which would allow natural recharge at a rate dependent on the hydraulic K and computed flow gradients.

During post-closure period, the following boundary conditions were changed to simulate the new hydraulic conditions:

- > Fixed heads were removed at the top of North Cell and South Cell TSF because they were assumed to be drained and frozen;
- > Drain conditions were removed in each pit because they are no longer in dewatering;
- > Drain condition at Central Dike downstream (D/S) pond was removed because it will no longer be pumped during post-closure period;
- > Pumping of the two wells at East Dike will be stopped.

 SNC • LAVALIN	TECHNICAL NOTE Hydrogeological modelling for in-pit tailings deposition	Prepared by: E. Millet, G. Comeau Reviewed by: C. Belanger, H. Sangam		
		Rev.	Date	Page
	SNC No. 651196-3000-4WER-0001 AEM No. 6118-E-132-001-TCR-003	A00	August 16 th , 2018	25

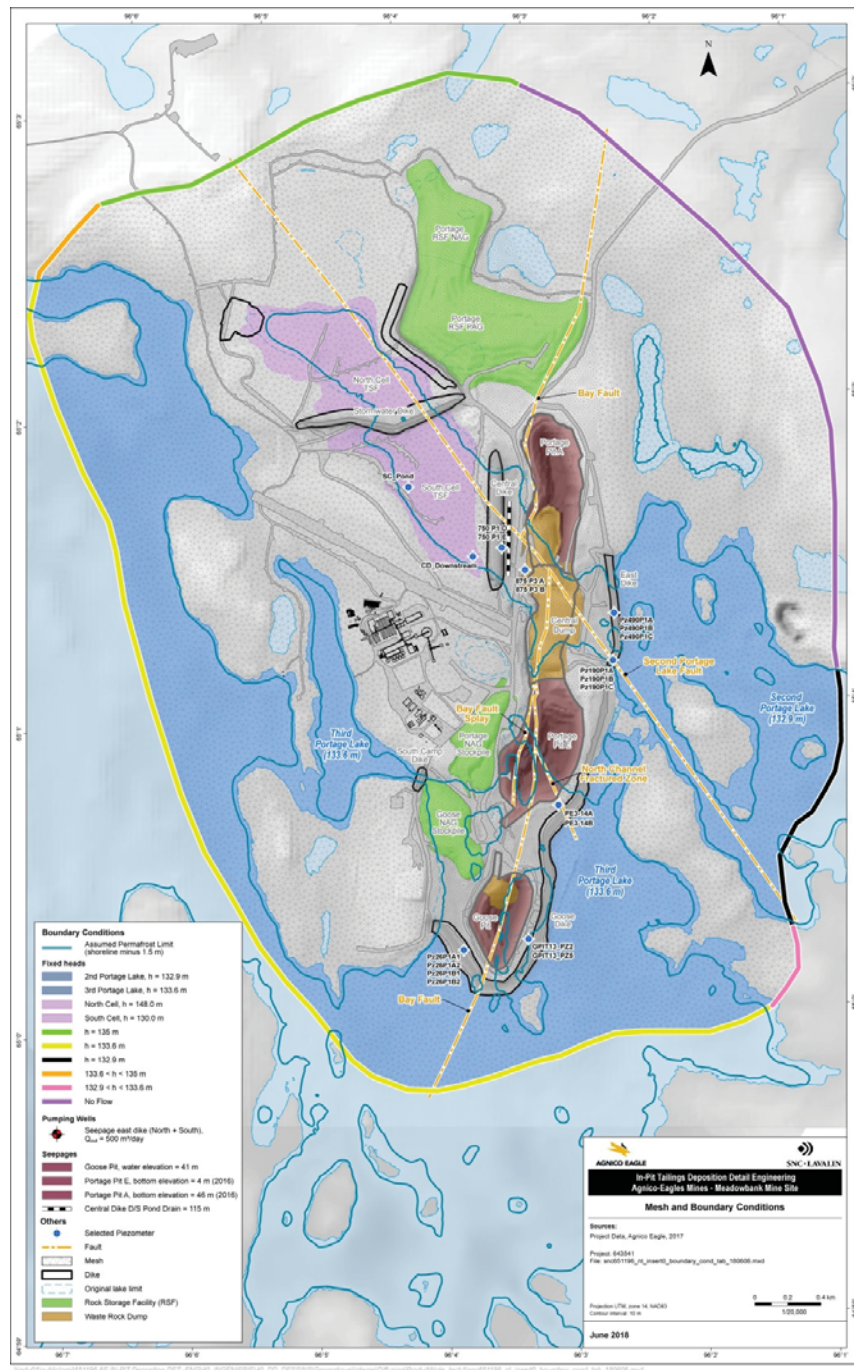



Figure 13 : Mesh and boundary conditions

 SNC • LAVALIN	TECHNICAL NOTE		Prepared by: E. Millet, G. Comeau Reviewed by: C.Belanger, H.Sangam		
	Hydrogeological modelling for in-pit tailings deposition		Rev.	Date	Page
	SNC No. 651196-3000-4WER-0001 AEM No. 6118-E-132-001-TCR-003		A00	August 16 th , 2018	26

3.3 Hydrogeological units


3.3.1 Hydraulic conductivity available data

An extensive set of hydraulic conductivity data were used to support the numerical model. Most of the data are included within a 150 m depth, corresponding to overall pit depths.

These data can be separated into the following sets. Figure 16 shows the location of the packer test data from which these values originate from:

- > Before 2017: 226 in-situ permeability tests (including packer tests and slug tests) conducted at 69 borehole locations. Each of these hydraulic conductivity values is related to a geological unit.
- > From summer 2017 field investigation: 48 packer tests conducted at 4 borehole locations located along anticipated migration paths from the pits to the lakes. Boreholes IPD-17-01 and IPD-17-02 are located between Central Dump and East Dike as whereas boreholes IPD-17-06 and IPD-17-07 are located from one side to another of Goose Pit.

Figure 14 presents the range of hydraulic conductivity values associated with each rock unit. No clear lithology-based classification was evident. Hence, all hydraulic conductivity values were then plotted against their arithmetic mean tested depth interval (Figure 15a). The data were also assessed separately, based on their spatial location (Figure 15b), but they didn't reveal any local trend. However, the bedrock hydraulic conductivity was found to generally decrease with depth as identified in previous hydrogeological studies (Golder, 2004) and with updated graphs (Figure 15a&b). Observed geometric mean bedrock hydraulic conductivities decreases from 10^{-7} m/s between 5 to 60 mbgs and to 10^{-8} m/s between 60 to 150 mbgs (Table 1). Values were then grouped in several overlaying units to define the model hydrogeological units or hydrostratigraphy.

 SNC • LAVALIN	TECHNICAL NOTE Hydrogeological modelling for in-pit tailings deposition	Prepared by: E. Millet, G. Comeau Reviewed by: C.Belanger, H.Sangam		
		Rev.	Date	Page
	SNC No. 651196-3000-4WER-0001 AEM No. 6118-E-132-001-TCR-003	A00	August 16 th , 2018	27

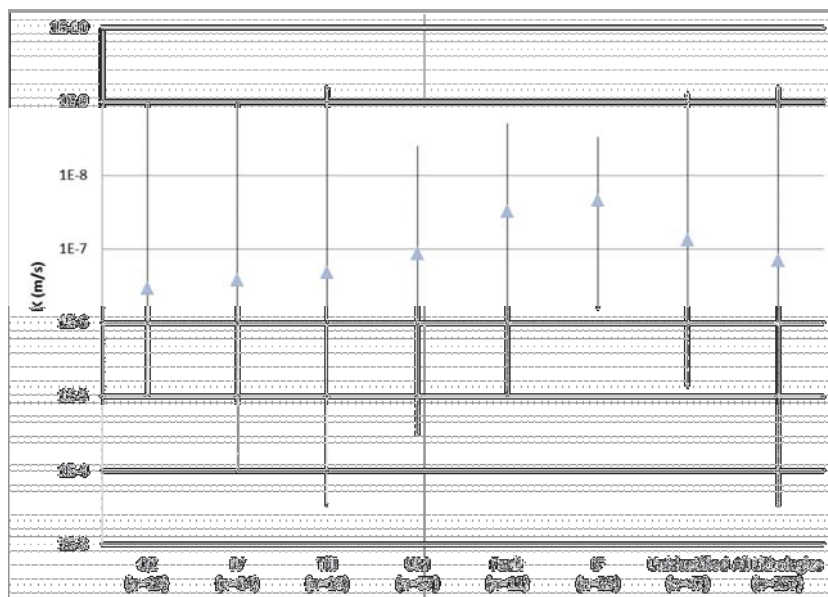


Figure 14 : Ranges and geometric mean of hydraulic conductivities by geological units

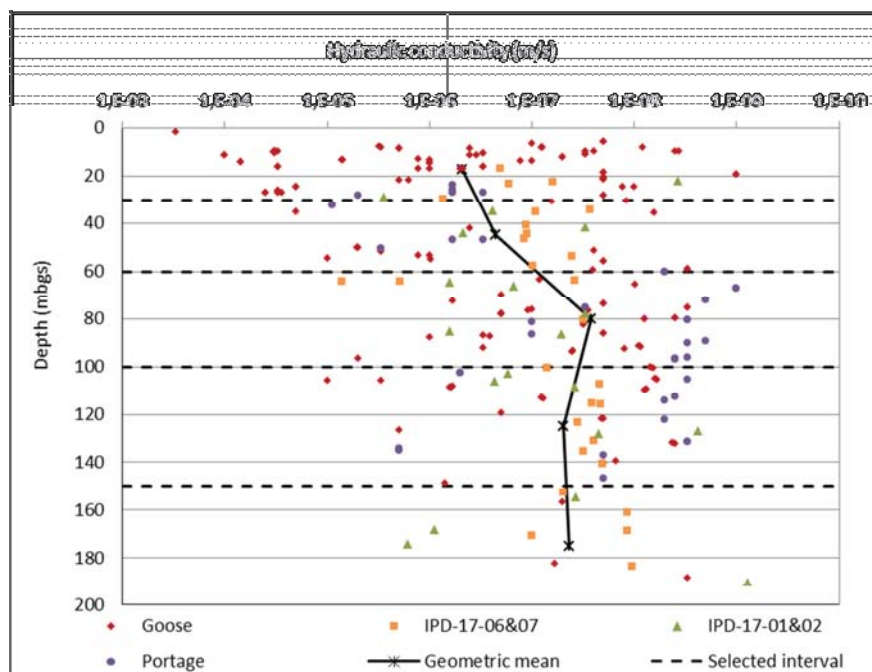



Figure 15: Hydraulic conductivity values versus depth with IPD-2017 boreholes

 SNC • LAVALIN	TECHNICAL NOTE		Prepared by: E. Millet, G. Comeau		
	Hydrogeological modelling for in-pit tailings deposition		Reviewed by: C.Belanger, H.Sangam		
			Rev.	Date	Page
	SNC No. 651196-3000-4WER-0001 AEM No. 6118-E-132-001-TCR-003		A00	August 16 th , 2018	28

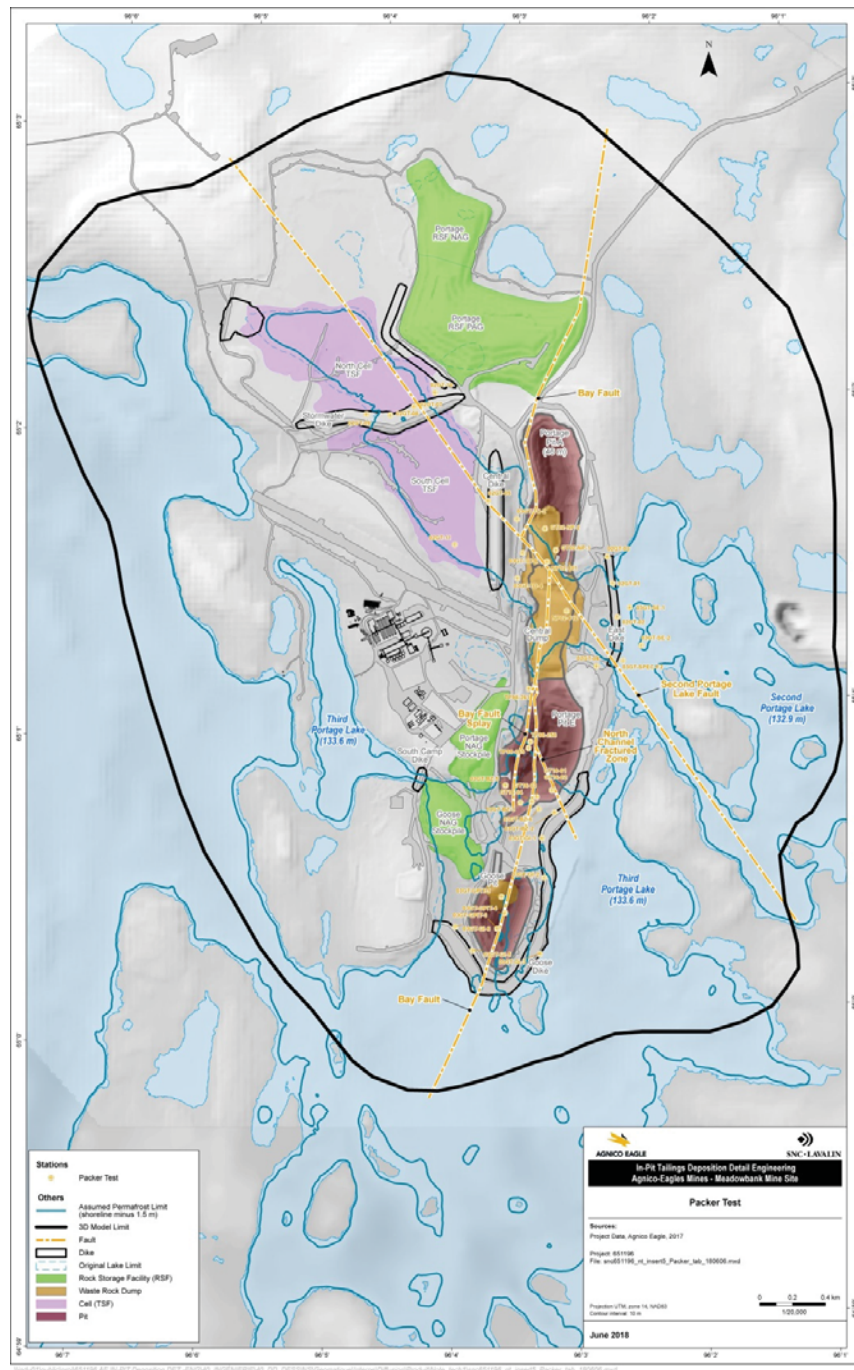




Figure 16 : Packer test locations

 SNC • LAVALIN	TECHNICAL NOTE		Prepared by: E. Millet, G. Comeau Reviewed by: C. Belanger, H. Sangam		
	Hydrogeological modelling for in-pit tailings deposition		Rev.	Date	Page
	SNC No. 651196-3000-4WER-0001 AEM No. 6118-E-132-001-TCR-003		A00	August 16 th , 2018	29

3.3.2 Hydrostratigraphy

In addition to the depth-based hydraulic conductivity units, all major structures which could affect the groundwater flow system were included in the hydrostratigraphy. Indeed, seepage and preferential flow areas have been identified in previous studies, including 2017 IPD boreholes results and are presented in the following section. Based on the observed hydraulic conductivity data as well as on literature values, hydraulic conductivities were associated to each of the following units and are summarized in Table 1.

- > **Overburden (till):** the project area is covered laterally by deposits of glacial till. This till unit can be described as a sandy till, having a fines (silt and clay) content of 30% to 40%, based on grain size analysis (Golder, 2005). In addition to till deposits, local occurrences of glaciofluvial sands and gravels have been noted. Till has been observed in the Central Dike area (Golder, 2008a) and at the lake bottoms. Lakebed sediments can reach several meters in thickness (Cumberland Resources Ltd, 2005b). The available data obtained from AEM indicated that the till thickness at the contact zone of till and bedrock varies from 2.5 to 7 m, with an arithmetic mean value of 5.3 m;
- > **Weathered bedrock:** the upper 10 to 30 m of the bedrock, is typically the portion of bedrock subjected to freeze/thaw cycles (Golder, 2016a);
- > **Competent bedrock:** Iron formations (IF), intermediate volcanics (IV) and ultramafic volcanics (UV) are the three main rock types characterized by a wide range of hydraulic conductivity values with data limited to the first 200 m depth. Below 200 m depth, the bedrock is assumed to be less permeable than the overlying units;
- > **Second Portage Fault:** follows the former Second Portage Lake arm, beneath the North Cell, South Cell, Central Dike, Central Dump and East Dike. This fault trends to the southeast and dips at 70 degrees to the southwest. As shown in Table 1, the hydraulic conductivities in areas with faults were found to be one or two orders of magnitude higher than the surrounding rock formations. Fractured rock associated with the Second Portage Lake Fault was assumed to have a hydraulic conductivity value of about 5×10^{-6} m/s near the surface (above 150 mbgs). Below 150 mbgs, hydraulic conductivity of the fault would be expected to be lower (Golder Associated Ltd, 2005);
- > **Bay Fault:** oriented north-south is roughly parallel to East Dike and Goose Dike. This fault dips with a 70 degree angle to the west. Bay Fault extends northward along the western flank of the Portage Pit A deposit (Golder, 2005);
- > **Bay Fault Splay:** same dip and direction as Bay Fault, but shallower (Cumberland, 2005b). The Splay is located on the western wall of Pit E. No specific hydraulic conductivity data were available for the Splay;
- > **Quartzite / Ultramafic contact:** the contact, extending under Goose Dike, was represented in the hydrogeological model as a narrow linear structure similar to Second Portage Lake and Bay Faults. The contact geometry is reproduced from the AEM 3D geological block model. During the Prefeasibility Study (SNC, 2017), this contact had been identified as an important seepage area. Packer tests, realized at IPD-17-06 during the 2017 field study investigation, intercepted high permeable levels (up to 7.1×10^{-6} m/s) at that contact.
- > **Central Dump:** a highly permeable unit based on the material type (waste rock), grain size curves and typical literature K-values.
- > **North Channel fractured zone:** represents a 50 m depth zone of relatively low rock mass quality on the south-east face of Pit E. The ultramafic rock forming the south wall is also serpentinized, and

 SNC • LAVALIN	TECHNICAL NOTE		Prepared by: E. Millet, G. Comeau Reviewed by: C.Belanger, H.Sangam		
	Hydrogeological modelling for in-pit tailings deposition		Rev.	Date	Page
	SNC No. 651196-3000-4WER-0001 AEM No. 6118-E-132-001-TCR-003		A00	August 16 th , 2018	30

appears to have significant proportions of the mineral talc. This contact has been characterized by Tetrattech (2016) as a seepage area. Twelve (12) packer tests were completed over selected intervals in four geotechnical boreholes. The packer testing results are generally consistent with a relatively intermediate to low hydraulic conductivity rock mass (Freeze and Cherry, 1979). The calculated hydraulic conductivity values range from 1×10^{-8} to 5×10^{-7} m/s without any strong correlation between test depth, lithology, or structure. In the model, this zone was represented following the southeastern wall of Pit E limited by the permafrost. Note that this seepage zone was only represented within the calibration model (2016) and not at post-closure because the contact was mined out during the Pit E southeastern wall pushback.

- > **Upper fractured bedrock under the Cells:** as confirmed by Golder (2017), the upper fractured bedrock under the Cells is highly permeable (2.0×10^{-3} m/s);
- > **Tailings:** According to ASTM D5084, constant head hydraulic conductivity tests were performed at three effective consolidation stresses: 100 kPa, 300 kPa, and 600 kPa. Respective hydraulic conductivities at standard temperature are 1.23×10^{-7} m/s, 8.01×10^{-8} m/s, and 6.30×10^{-8} m/s (Golder, 2017; Lab test tailings). The geometric mean value of 8.9×10^{-8} m/s was used as a reference in the model;
- > **TSF and Dewatering Dikes:** Low permeability cells have been used to represent dams with impervious cores in the model, such as Goose Dike, East Dike and South Camp Dike. Low permeability cells have also been used to represent Central Dike with an impervious liner on its upgradient side;
- > **Permafrost:** can be considered as a unique impermeable hydrostratigraphic unit. The permafrost delimitation is particularly important around Portage Pit A since the pit is almost entirely frozen.



 SNC • LAVALIN	TECHNICAL NOTE Hydrogeological modelling for in-pit tailings deposition	Prepared by: E. Millet, G. Comeau Reviewed by: C.Belanger, H.Sangam		
		Rev.	Date	Page
	SNC No. 651196-3000-4WER-0001 AEM No. 6118-E-132-001-TCR-003	A00	August 16 th , 2018	31

Table 1 : Hydrostratigraphic units and observed K values with depth

Hydrostratigraphic Unit	Depth (m)	Observed geometric mean K value (m/s)	Source
Till deposit	0 - 5	5.5×10^{-6}	Data before 2017
Weathered Rock	5 - 30	4.8×10^{-7}	Data before 2017 and Summer 2017 IPD boreholes
Competent Rock	30 - 60	2.3×10^{-7}	Data before 2017 and Summer 2017 IPD boreholes
Competent Rock	60 - 100	2.7×10^{-8}	Data before 2017 and Summer 2017 IPD boreholes
Competent Rock	100 - 150	4.9×10^{-8}	Data before 2017 and Summer 2017 IPD boreholes
Competent Rock	150 - 1000	Assumed low permeability (1.0×10^{-8})	n/a
Second Portage Fault	30 - 70	6.0×10^{-6}	Data before 2017
Bay Fault	60 - 180	1.4×10^{-8}	Data before 2017
Bay Fault Splay	5 - 50	Assumed equal to Bay Fault (1.4×10^{-8})	n/a
Ultramafic/Quartzite contact	5 - 165	7.1×10^{-6}	IPD-17-06, max value at 67 masl
Central Dump	5 - 165	Coarse-grained permeable material (Assumed = 1.0×10^{-3})	AEM
North channel fractured zone	0 - 100	8.2×10^{-8}	GT-16 geometric mean value. Tetrattech (2016)
Meadowbank TSF tailings and Amaruq in-pit tailings	0 - 30 0 - 140	8.9×10^{-8}	Golder (2017). Central Dike investigation. Golder (2017) Lab tests Geometric mean under different pressure values
Upper fractured bedrock under the Cells	30 - 35	2.0×10^{-3}	Golder (2017). Update on Central Dike assessment
Dikes	0 - 15	Low permeability (1.0×10^{-8})	Golder, 2017
Permafrost	0 - 300	Very low permeability, inactive cells	Morgenstern (1973)

 SNC • LAVALIN	TECHNICAL NOTE		Prepared by: E. Millet, G. Comeau Reviewed by: C.Belanger, H.Sangam		
	Hydrogeological modelling for in-pit tailings deposition		Rev.	Date	Page
	SNC No. 651196-3000-4WER-0001 AEM No. 6118-E-132-001-TCR-003		A00	August 16 th , 2018	32

3.4 Calibration

3.4.1 Conceptual groundwater model validation prior to calibration


In order to validate the hydrogeological conceptual model, a first simulation was run with initial hydraulic conductivity and without any active pumping or drains to obtain preliminary groundwater flow patterns. The groundwater flow was evaluated qualitatively to determine if this was in agreement with the conceptual model and with anticipated regional groundwater flow directions. This preliminary validation allowed representing the regional groundwater flow from the north-western boundary of the model toward the Second Portage Lake direction, which is the lowest hydraulic component of the system.

3.4.2 Calibration strategy and pumping rates

During the calibration process, the initial values of hydraulic conductivity were adjusted and the numerical model was run repeatedly until the model predictions reasonably matched the observed 2016 dewatering rates for each pit. Drain conditions at pit shells, pumping rates at Central Dike downstream (D/S) pond and at the 2 pumping wells located at East flat were reproduced during the calibration process. Due to the unavailability of natural hydraulic conditions and non-impacted (background) piezometric levels, the calibration was mainly carried out based on the 2016 discharge rates for each pit under steady-state conditions. Data from 2016 has been selected for model calibration since Portage Pit A and Portage Pit E's base elevation and assumed pumped water levels were relatively stable. The pit base elevations (and water elevation) were at 46 masl and 4 masl for Pit A and Pit E, respectively, as seen in Figure 17 and in the conceptual model during dewatering (Figure 9).

In order to have a representative hydrogeological model, calibration was achieved after adjustment of hydraulic conductivities and comparison of simulated pumping rates in each pit to the 2016 measured groundwater baseflow rates. Groundwater baseflow is a portion of the total pumping rate and corresponds to the contribution of groundwater seepage to the pits, regardless of the direct precipitation and runoff water portion that comes from the top of the pits. During winter months, precipitation (snow) is stored on the ground, surface water runoff is negligible, and thus the pumping rate could be considered equal to the groundwater contribution to the pit dewatering rates. Therefore, the 2016 winter months (October to May) have been selected to estimate the groundwater contribution to dewatering rates at each pit. Total monthly pumping rates for Goose Pit, Portage Pit A, Pit E as well as for Central Dike pond and East Dike North & South pumping wells were extracted from AEM's annual water balance and are presented in Figure 17.

Since Portage Pit A and Pit E pumping rates are not measured separately on the site, the combined Pit A and Pit E pumping rate was considered for calibration purposes. The equivalent daily total pumping rate from Portage Pit A and Pit E is 363 m³/day in 2016, from which 35% (127 m³/d) comes from groundwater. During 2016, Goose Pit filled at a rate of 1028 m³/day, with 35% (435 m³/day) of this water attributed to groundwater inflow. Water level rise and equivalent inflow rate were assumed equal to the volume that would have to be pumped out of Goose Pit. Central Dike downstream pond, East Dike North & South wells are pumping respectively at 12 771 m³/day and at 500 m³/day.

 SNC • LAVALIN	TECHNICAL NOTE	Prepared by: E. Millet, G. Comeau Reviewed by: C.Belanger, H.Sangam		
	Hydrogeological modelling for in-pit tailings deposition	Rev.	Date	Page
	SNC No. 651196-3000-4WER-0001 AEM No. 6118-E-132-001-TCR-003	A00	August 16 th , 2018	33

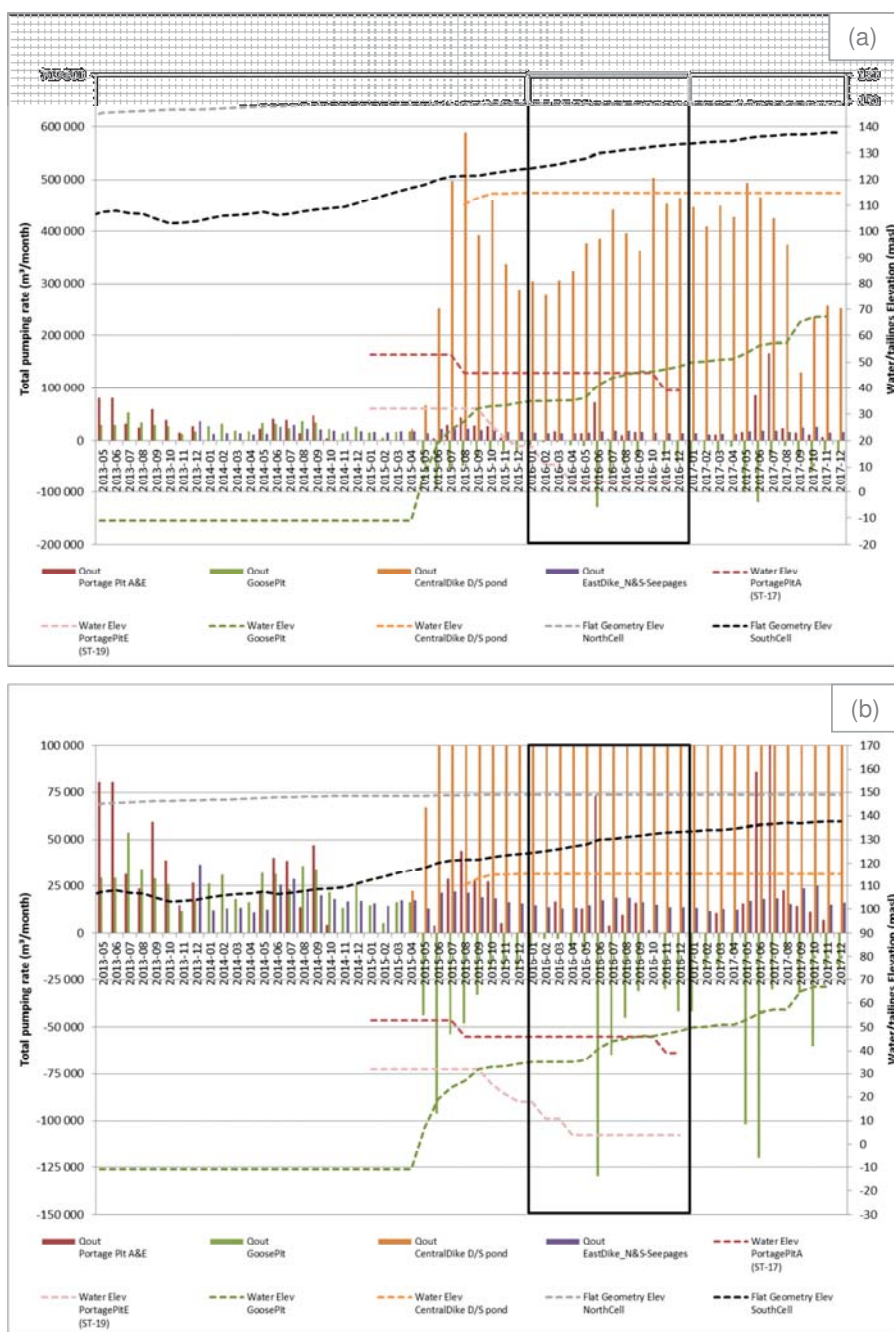


Figure 17 : Measured monthly total pumping rate (2013-2017) (b) is a zoomed-in view of (a)


 SNC • LAVALIN	TECHNICAL NOTE Hydrogeological modelling for in-pit tailings deposition	Prepared by: E. Millet, G. Comeau Reviewed by: C.Belanger, H.Sangam		
		Rev.	Date	Page
	SNC No. 651196-3000-4WER-0001 AEM No. 6118-E-132-001-TCR-003	A00	August 16 th , 2018	34

Table 2 : 2016 Total pumping rate and groundwater contribution to pit dewatering

Pumping	Measured total pumping rate (m ³ /d)	Measured GW inflow rate (m ³ /d)	GW contribution to total pumping rate (%)
Portage Pit A & Pit E	-363	-127	35
Goose Pit*	-1028	-435	42
Central Dike drain (pond)	-12 771	-12 771	100
East Dike North (EDN)	-500	-250	100
East Dike South (EDS)		-250	100

Note : * : Goose Pit water level is rising since dewatering has stopped. GW inflow is considered equal to dewatering rate.

3.4.3 Calibrated hydraulic conductivities and simulated pumping rates

Table 4 presents a comparison between the estimated total flow rate including groundwater flow and the FEFLOW model-calibrated pit inflow. Calibrated Portage Pit A, Goose Pit and Central Dike D/S pond inflows are reasonable since the ratios between estimated and simulated values are close to 1.0.

Hydraulic conductivities were adjusted within reasonable ranges to simulate the observed 2016 annual groundwater contribution to the water inflow at each pit, Central Dike D/S Pond and East Dike pumping well. Table 3 compares the calibrated hydraulic conductivity of each hydrostratigraphic unit to their initial values. Fault hydraulic conductivities have generally been increased by 0.5 orders of magnitude to represent the dewatering rates. Bedrock hydraulic conductivities have been slightly lowered, especially between 30 and 60 mbgs (layers 12 to 17). The hydraulic conductivity from other units remained relatively intact. The sensitivity of these changes will be discussed later in the sensitivity analysis.

Details of calibrated hydraulic conductivities with hydrostratigraphic units and depth are also provided in Table A.1, Appendix A.


 SNC • LAVALIN	TECHNICAL NOTE Hydrogeological modelling for in-pit tailings deposition	Prepared by: E. Millet, G. Comeau Reviewed by: C.Belanger, H.Sangam		
		Rev.	Date	Page
	SNC No. 651196-3000-4WER-0001 AEM No. 6118-E-132-001-TCR-003	A00	August 16 th , 2018	35

Table 3 : Distribution of calibrated hydraulic conductivity for each unit of the model

Unit	Layers	Initial K value (m/s)	Calibrated hydraulic conductivity (m/s)
Till deposit	1 to 4	5.5×10^{-6}	5×10^{-6}
Weathered bedrock (5-30m)	5 to 11	4.8×10^{-7}	1.7×10^{-7}
Competent bedrock (30-60m)	12 to 17	2.3×10^{-7}	4.2×10^{-8}
Competent bedrock (60-100m)	18 to 24	2.7×10^{-8}	2.7×10^{-8}
Competent bedrock (100-150m)	25 to 31	4.9×10^{-8}	1.8×10^{-8}
Competent bedrock (150-1000m)	32 to 50	1.0×10^{-8}	1.0×10^{-8}
Ultramafic/Quartzite contact	6 to 34	7.1×10^{-6}	2.0×10^{-6}
North channel fractured zone	n/a	8.2×10^{-8}	5.0×10^{-7}
Second Portage Fault	5 to 39	6.0×10^{-6}	1.5×10^{-5}
	40 to 50		1.0×10^{-6}
Bay Fault	5 to 39	1.4×10^{-8}	6.0×10^{-7}
	40 to 50		4.0×10^{-8}
Bay Fault Splay	5 to 18	Assumed equal to Bay Fault (1.4×10^{-8})a	6.0×10^{-7}
Portage Central Dump	1 to 19	Assumed coarse-grained permeable material (1.0×10^{-3})	1.0×10^{-3}
Upper fractured bedrock below the cells	4	2.0×10^{-3}	1.1×10^{-3}
TSF North Cell & South Cell tailings	1 to 3	1.0×10^{-7}	1.0×10^{-7}
In-pit tailings	4 to 32 (at Pit E location)	8.9×10^{-8}	1.0×10^{-7}
Dikes	1 to 7	Low permeability (1.0×10^{-8})	1.0×10^{-8}
Permafrost	1 to 39	Very low permeability (Inactive cells)	Inactive cells


 SNC • LAVALIN	TECHNICAL NOTE Hydrogeological modelling for in-pit tailings deposition	Prepared by: E. Millet, G. Comeau Reviewed by: C.Belanger, H.Sangam		
		Rev.	Date	Page
	SNC No. 651196-3000-4WER-0001 AEM No. 6118-E-132-001-TCR-003	A00	August 16 th , 2018	36

Table 4 : Calibration results on GW inflow rates during dewatering

Pumping	Measured GW inflow rate (m ³ /d)	Calibrated GW inflow rate (m ³ /d)	Simulated / Measured GW inflow ratio
Portage Pit A and Pit E	-127	-196	1.5
Goose Pit	-435	-423	1.0
Central Dike drain	-12 771	-12 383	1.0
EDN	-250	-250	1.0
EDS	-250	-250	1.0


3.4.4 Simulated water levels

Although if water levels were not used for model piez calibration during dewatering operations, simulated hydraulic heads were also compared with selected 2016 piezometric data in order to cover multiple areas of the mine site (South Cell TSF, Central Dike, East Dike, Portage Pit E and Goose Pit).

Approximately 100 vibrating wire piezometer (VWP) multi-level stations are available at the Meadowbank mine site. The VWPs are mostly installed in dikes and are close to lakes and dewatered pits. Because of the close proximity of the lakes, which act as constant head boundaries to the dewatered pits, the hydraulic head variation is significant over the short horizontal distance. For example, over the 200 m distance between Third Portage Lake and the bottom of Goose Pit, water elevation drops from 133.6 masl to 48 masl (end of 2016 water level), resulting in an estimated hydraulic gradient of 0.4 m/m. Consequently, a small difference in VWP location could lead to high discrepancies between observed and simulated hydraulic heads. Nevertheless, simulated and observed hydraulic heads have been compared to give an appreciation of the calibration results under dewatering conditions.

A total of 20 VWPs at 9 multi-level stations were selected to cover the main areas of the mine site (South Cell TSF, Central Dike, East Dike, Portage Pit E and Goose Pit) and their locations are shown in Figure 13. Comparisons between observed and simulated hydraulic heads are available in Figure 18. Except for PE3-14A&B (in Pit E south-east wall) that are highly offset from the calibration line, the greatest differences are on the order of 8 m and occur at Goose Pit (Pz26 series) and East Dike location (Pz490 series). Discrepancies in PE3-14A&B simulated vs observed water levels might be explained by mining activities and southeast wall pushback occurring in Pit E in 2016. The Root Mean Square Error (RMSE) for the selected VWP data is 9 %, which represent an acceptable value considering the high hydraulic head variation. Normally, the industry standard accepts a RMSE under 15% although the target is less than 10%. Simulated versus observed hydraulic heads at VWP location is found in Table A.2, Appendix A.

Figure 19a and b map regional simulated hydraulic heads for the base case at the top of the model (Slice 6) and the bottom (Slice 44) (below permafrost) during 2016 dewatering operations. The white zone represents permafrost areas. At the top of the model, the groundwater flow system is consistent with the conceptual hydrogeological model under dewatering conditions, with groundwater diverted to the center of each pit. Pit dewatering also has impacts on the deep groundwater flow regime and groundwater is directed toward the pits. Higher hydraulic heads are also represented at the North and South Cells of the TSF, where the higher tailings and reclaim water

 SNC • LAVALIN	TECHNICAL NOTE Hydrogeological modelling for in-pit tailings deposition	Prepared by: E. Millet, G. Comeau Reviewed by: C. Belanger, H. Sangam		
		Rev.	Date	Page
	SNC No. 651196-3000-4WER-0001 AEM No. 6118-E-132-001-TCR-003	A00	August 16 th , 2018	37

elevations have created a hydraulic dome. It is important to note that Second and Third Portage Lake water levels remain constant, along with the North Cell and South Cell hydraulic heads, which were also fixed for this base case simulation of pit dewatering.

Before and after calibration of the groundwater flow model, a simulation was also carried out without pit dewatering and with the boundary conditions presented at Figure 13 to verify that the modelling is consistent with the conceptual representation of the natural regional groundwater flow regime. Figure 19c and d illustrate the calibrated hydraulic heads at the top (Slice 6) and the bottom (Slice 44) of the model. The equipotential lines are consistent with the regional groundwater flow system that extends from the northwest to the southeastern area of the model extension. This behavior can also be represented along a cross-section (Figure 20) that was traced along the flow direction (Figure 19c and d).

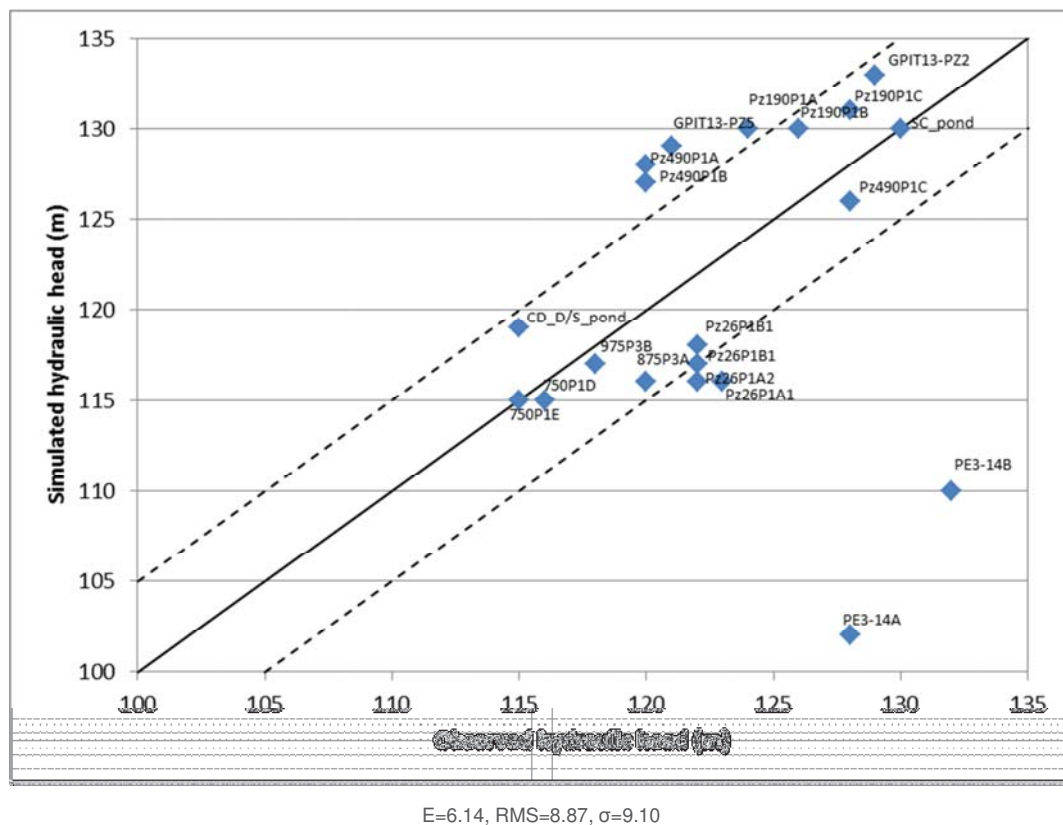



Figure 18 : Comparison of simulated and observed hydraulic heads during pit dewatering

 SNC • LAVALIN	TECHNICAL NOTE	Prepared by: E. Millet, G. Comeau		
	Hydrogeological modelling for in-pit tailings deposition	Reviewed by: C.Belanger, H.Sangam		
		Rev.	Date	Page
	SNC No. 651196-3000-4WER-0001 AEM No. 6118-E-132-001-TCR-003	A00	August 16 th , 2018	38

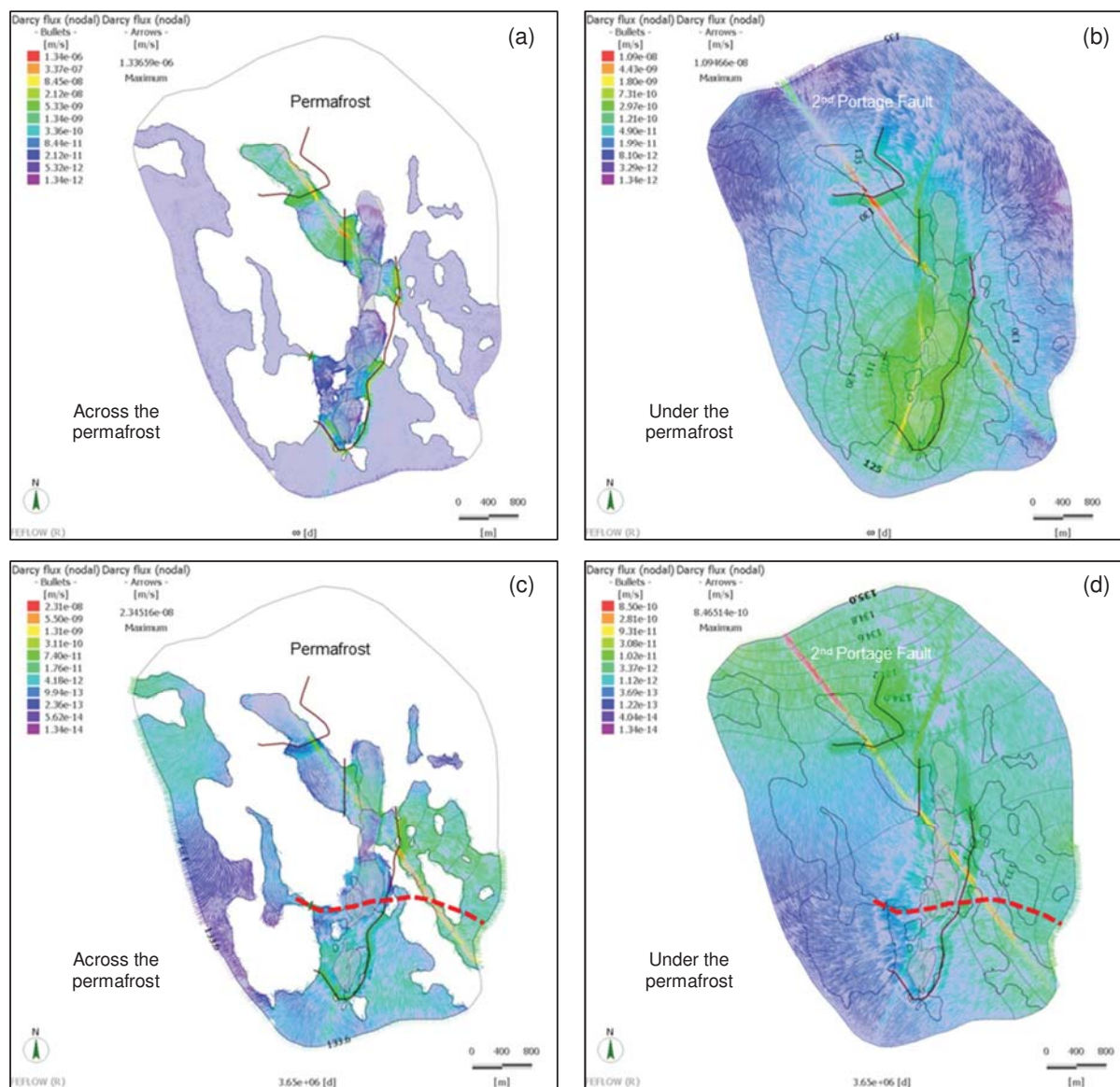


Figure 19 : Darcy flux (m/s) and calibrated hydraulic heads (masl) under dewatering conditions (a) for slice 6 (elevation 120 to 130 m) and (b) for slice 44 (elevation at -500 m); and under natural conditions (c) for slice 6 (elevation 120 to 130 m) and (d) for slice 44 (elevation at -500 m). The dashed line represents the conceptual cross-section location of Figure 20.

 SNC • LAVALIN	TECHNICAL NOTE Hydrogeological modelling for in-pit tailings deposition	Prepared by: E. Millet, G. Comeau Reviewed by: C. Belanger, H. Sangam		
		Rev.	Date	Page
	SNC No. 651196-3000-4WER-0001 AEM No. 6118-E-132-001-TCR-003	A00	August 16 th , 2018	39

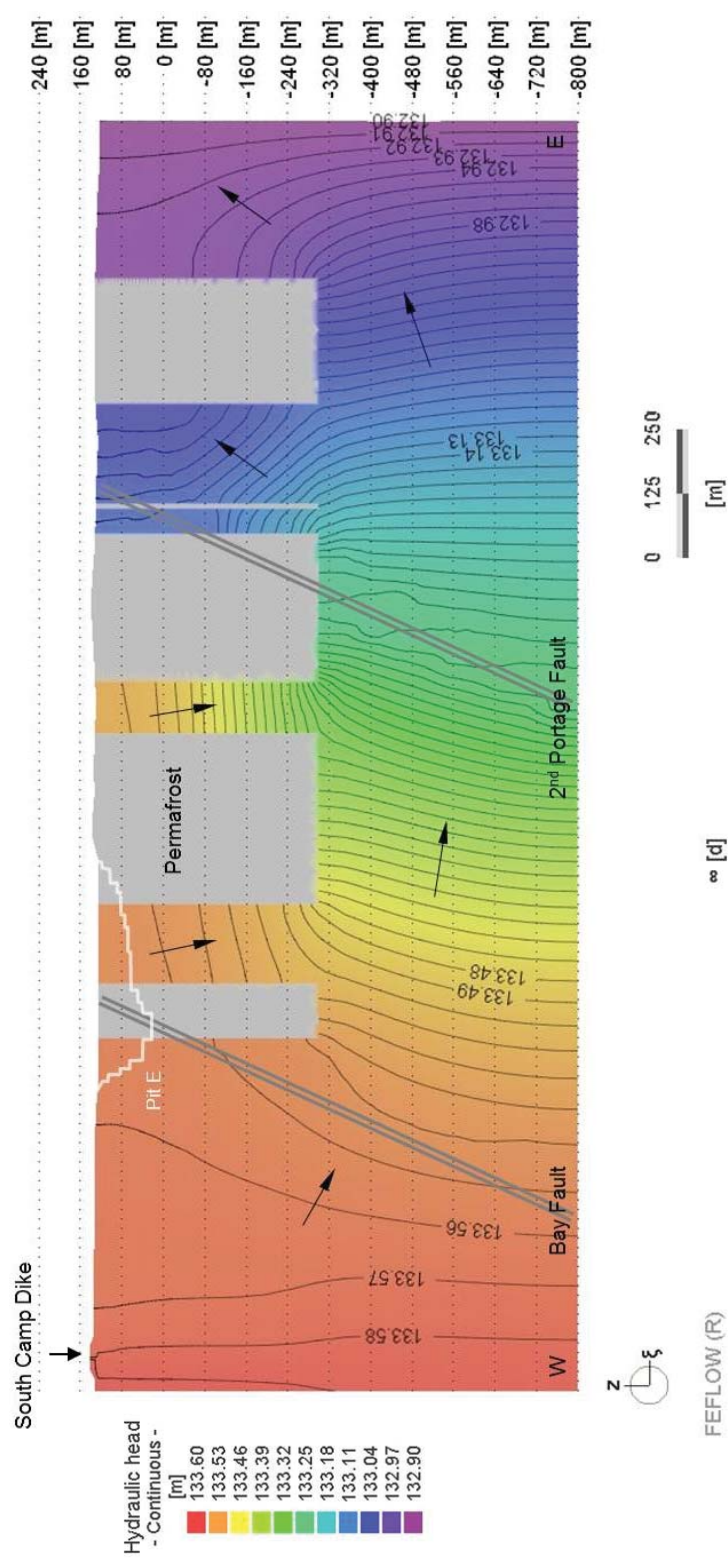



Figure 20 : Hydraulic heads under natural conditions (trace located on Figure 19)

 SNC • LAVALIN	TECHNICAL NOTE Hydrogeological modelling for in-pit tailings deposition		Prepared by: E. Millet, G. Comeau Reviewed by: C.Belanger, H.Sangam	
			Rev.	Date
	SNC No. 651196-3000-4WER-0001 AEM No. 6118-E-132-001-TCR-003		A00	August 16 th , 2018
				Page 40

3.5 Sensitivity analysis on flow parameters

A sensitivity analysis of a hydrogeological model helps define which of the model parameters has the most influence on the modelling results. It can also be used to adapt the calibration strategy or to validate if some insufficient data will have a great impact on modelling results. The selected parameters for this sensitivity analysis are:

- > Fault hydraulic conductivities (K-value);
- > Quartzite/Ultramafic contact (K-value);
- > Competent bedrock (K-value);
- > Upper fractured bedrock (K-value) at former Second Portage Lake arm (at North & South Cells location).

Modelled flow rates after variation of these parameters were compared to the calibrated flow rates of the base case scenario of the 2016 pit dewatering as shown in Table 5.

Based on this sensitivity analysis, the till and upper fractured bedrock hydraulic conductivity have a major impact on the simulated pumping (dewatering) rate at Central Dike D/S pond, increasing the flow rate by 1.9 times if its hydraulic conductivity is doubled. On the other hand, increasing the tailings hydraulic conductivity by a factor of 2 has a limited effect on the Central Dike D/S pond pumping rate. The quartzite-ultramafic contact also leads to a 1.6 times greater inflow into Goose Pit if its hydraulic conductivity is doubled. Also, the hydraulic conductivity of the small permafrost zone at the southwestern end of Portage Pit A has a great impact on simulated groundwater inflow to the same pit.

Minor changes have been observed with the increase of fault hydraulic conductivity for all pits. As presented in the PFS modelling work (SLI, 2017), an increase in water level of Third Portage Lake also has little effect on pit inflows. According to AEM data, lake levels vary from 132.4 to 133.4 masl for Second Portage Lake and from 133.1 to 134.1 masl for Third Portage Lake.


 SNC • LAVALIN	TECHNICAL NOTE		Prepared by: E. Millet, G. Comeau Reviewed by: C.Belanger, H.Sangam		
	Hydrogeological modelling for in-pit tailings deposition		Rev.	Date	Page
	SNC No. 651196-3000-4WER-0001 AEM No. 6118-E-132-001-TCR-003		A00	August 16 th , 2018	41


Table 5 : Sensitivity analysis results for the flow model

Hydraulic conductivity of	Factor	Location	Measured Flow Rate (m ³ /d)	Modelled Flow Rate from sensitivity analysis (m ³ /d)	Ratio (Modelled/Measured)
Base Case	-	Pit A & E	-127	-196	1.5
		Goose Pit	-435	-423	1.0
		Central Dike Drain	-12 771	-12 383	1.0
Faults & Ultramafic/Quartzite contact	K multiplied by 2	Pit A & E	-127	-325	2.6
		Goose Pit	-435	-697	1.6
		Central Dike Drain	-12 771	-13 042	1.0
Fractured Bedrock	K multiplied by 2	Pit A & E	-127	-253	2.0
		Goose Pit	-435	-473	1.1
		Central Dike Drain	-12 771	-12 779	1.0
Upper fractured bedrock under North & South Cells	K multiplied by 2	Pit A & E	-127	-213	1.7
		Goose Pit	-435	-426	1.0
		Central Dike Drain	-12 771	-23 925	1.9

4.0 CONTAMINANT TRANSPORT MODELLING

The study undertaken for the water quality forecast at closure (SLI, 2018a) shows that treatment of the water cover will be required at this period. Then, Goose Dike will be breached, creating a water cover, a well-known method to limit the generation of acid mine drainage (AMD) (Vigneault et al., 2001; Kachhwal et al., 2011; Awoh, 2012; Moncur et al., 2015). Thus, pit lakes were not considered as a contaminant source in the hydrogeological modelling.

The following sections present the conceptual model used to simulate contaminant transport in groundwater at closure and the associated transport parameters. One of the modelling objectives was to evaluate the arrival time and concentrations of contaminants to the lake. This has been assessed with simulation results for two contaminants of concern.

 SNC • LAVALIN	TECHNICAL NOTE Hydrogeological modelling for in-pit tailings deposition	Prepared by: E. Millet, G. Comeau Reviewed by: C.Belanger, H.Sangam		
		Rev.	Date	Page
	SNC No. 651196-3000-4WER-0001 AEM No. 6118-E-132-001-TCR-003	A00	August 16 th , 2018	42

4.1 Contaminant transport conceptual model

Bethke (1996) mentions that to be successful, a geochemical conceptual model should portray the important features of the problem of interest without necessarily attempting to reproduce each chemical or mineralogical detail. To create a useful conceptual model, we needed to evaluate the initial conditions and composition of the system as well as the reaction process envisioned.

This problem can be conceptualized in two related parts (Figure 21):

1. The contaminant source or the initial geochemical conditions occurring in the pits and,
2. The contaminant plume or the migration of dissolved species within the bedrock along flowpaths.

In both cases, the behavior of the source and the plume will depend on a set of physical and chemical processes. In terms of physical process, the groundwater flow system, through advection and dispersion, is the main driving force of contaminant transport. Molecular diffusion can also play an important role where flow velocities are low. High hydraulic gradients will wash off the source and increase the migration rate of the contaminant faster than with a low hydraulic gradient.

Chemical reactions like oxidation, precipitation or adsorption will also influence contaminant migration by reducing or increasing their mass in the groundwater. These chemical processes are related to the specific contaminant of concern and also on the geochemical context. Since chemical processes involving oxidation and precipitation are difficult to reproduce without strong supporting data, a realistic but simplified conceptual model has been designed which does not aim to reproduce these specific reactions. Limitations and assumptions in the conceptual model are also identified below.

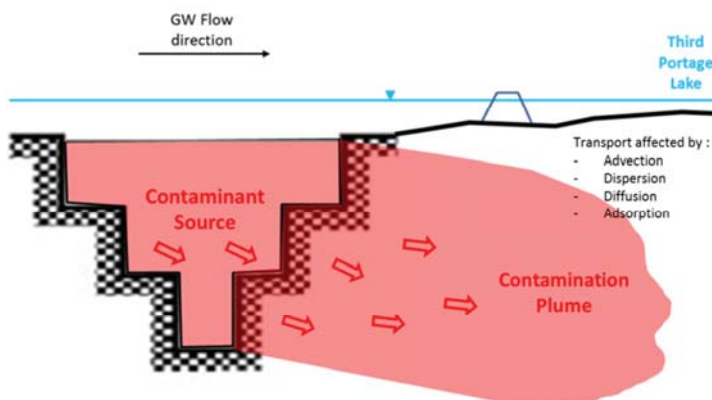



Figure 21: Conceptual transport model

The following sections will present the contaminant transport conceptual model, transport parameters used in the 3D model, simulation results for two contaminants of concern and finally, in order to evaluate the uncertainty arising from the parameters choices, a sensitivity analysis will be detailed.

 SNC • LAVALIN	TECHNICAL NOTE		Prepared by: E. Millet, G. Comeau Reviewed by: C. Belanger, H. Sangam		
	Hydrogeological modelling for in-pit tailings deposition		Rev.	Date	Page
	SNC No. 651196-3000-4WER-0001 AEM No. 6118-E-132-001-TCR-003		A00	August 16 th , 2018	43

4.1.1 Contaminants of concern

Two (2) contaminants of concern were chosen for the transport simulations: chloride and arsenic. These two chemical parameters are typically found in reclaim water geochemical signatures. An in-pit water quality assessment at closure has been produced during the In-Pit Tailings Deposition Detailed Engineering project (SLI, 2018a) and shows the expected untreated concentrations of each pit lake, and thus tailings pore water (Table A.3, Appendix A). Each chemical parameter, found in each untreated pit lake, is compared with the CCME guideline for the Long-term Aquatic Life Protection for fresh water.


Chloride was selected since it is a non-reactive tracer and will follow the pathway and velocity of groundwater. Arsenic was also selected for transport simulations as it is a well-known toxic compound, it is exceeding the CCME criteria at the pit source, if untreated, (Figure A.3, Appendix A) and it is less retarded than others (Figure A.4, Appendix A). Partition coefficient (K_d) and retardation factor (R) will be explained below.

Chloride

Sodium chloride (NaCl) is a naturally occurring element ubiquitous in the environment. Sodium (Na) is the sixth most abundant element in the Earth's crust and the most abundant cation in the hydrosphere (the hydrosphere is all water, including atmospheric and oceanic water, on Earth; Gornitz, 1972). Chloride has been shown to be a nonreactive solute in a wide range of groundwater settings (Davis et al., 1980). Dissolved NaCl is considered to be a conservative tracer meaning it will behave like water. Literature on the adsorption of chloride shows no or very little adsorption (EPA, 1996). Conservative tracers are useful for tracking flowpaths through groundwater and understanding physical transport phenomena.

Arsenic

Arsenic is a known carcinogen, and occurs in natural systems in the +5 (arsenate) and +3 (arsenite) valence states. Arsenic (III), As^{3+} , is more mobile and is many times more toxic than As^{5+} . Arsenates are the predominant species in oxygenated waters, whereas arsenite species predominate under anoxic or reduced conditions (Fields et al. 2000), which are similar to those found under a water cover. The pH and redox conditions are the two most important geochemical factors affecting the mobility of arsenic in the environment. Relative to the other elements, arsenic is among the most problematic in the environment because of its relative mobility over a wide range of redox conditions (Smedley, 2001) as shown in Figure 22.

 SNC • LAVALIN	TECHNICAL NOTE Hydrogeological modelling for in-pit tailings deposition	Prepared by: E. Millet, G. Comeau Reviewed by: C.Belanger, H.Sangam		
		Rev.	Date	Page
	SNC No. 651196-3000-4WER-0001 AEM No. 6118-E-132-001-TCR-003	A00	August 16 th , 2018	44

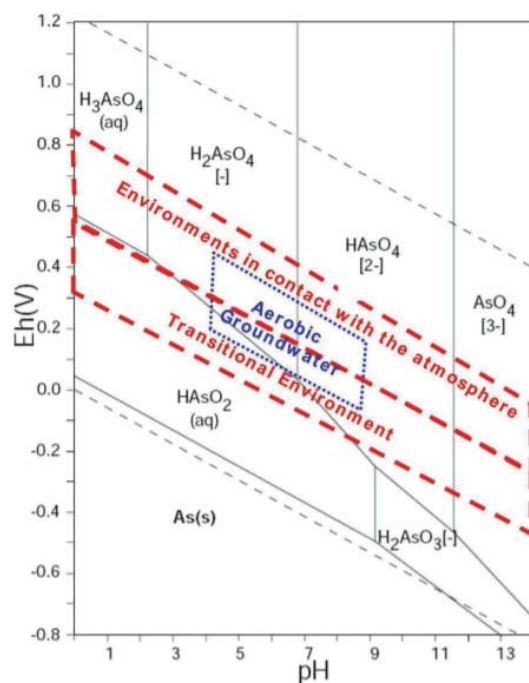


Figure 22: Arsenic speciation in groundwater regimes (API, 2011)

4.1.2 Source representation

Initial concentrations of chloride and arsenic in the in-pit tailings pore water

Initial concentration of chloride and arsenic in tailings pore water was based on the in-pit water quality assessment at closure (SLI, 2018a) which doesn't account for any treatment of that pore water. Table 6 shows the chloride and arsenic concentrations used as the initial source concentration for each pit (initial concentration C_i). The CCME water quality guidelines for long-term protection of aquatic life in fresh water are also given for each contaminant. The chloride concentration at Pit A (116 mg/L) and Pit E (141 mg/L) are close to the guideline while it is lower at Goose Pit (22 mg/L) because process water is transferred from Goose Pit to Pit A and E. Other reclaim water chemical parameters can be found in Table A.3 (Appendix A) and are also compared to CCME guidelines.


 SNC • LAVALIN	TECHNICAL NOTE		Prepared by: E. Millet, G. Comeau Reviewed by: C. Belanger, H. Sangam		
	Hydrogeological modelling for in-pit tailings deposition		Rev.	Date	Page
	SNC No. 651196-3000-4WER-0001 AEM No. 6118-E-132-001-TCR-003		A00	August 16 th , 2018	45

Table 6 : Initial concentrations C_i of tailings pore water as predicted by the in-pit water quality assessment at closure report (SLI, 2018a)

Parameter	Unit	CCME Guideline	C_i Pit A	C_i Pit E	C_i Goose Pit
Chloride (Cl^-)	mg/L	120	116	141	22
Arsenic (As^{3+} or As^{5+})	mg/L	0.005	0.9	1.1	0.15

Source concentration against time


The contaminant source is considered as the reclaim water that is trapped in the matrix of the tailings, e.g. located in the in-pit tailings pore water. After the deposition, tailings pore water concentrations will typically decrease from its initial concentration C_i to reach a residual and lower concentration. Based on the literature, the residual concentration will normally be reached after flushing the tailings with three (3) pore volumes (MEND, 2000). One of the most important questions regarding the source kinetics is how long will it take for the contaminant to reach this residual concentration.

The time to flush three (3) pore volumes is based on the groundwater velocity through the pit. Based on the FEFLOW model, velocities are very low. For example, the hydraulic gradient at Goose Pit is less than 0.00005 m/m. Consequently, the time to flush three (3) pore volumes will be very long (almost 60 000 years as shown in Table 7). Therefore, it appears that simulating a constant source over time will be conceptually justified with the low hydraulic gradient expected at Meadowbank site during post-closure period.

Table 7 : Time for three (3) tailings pore volumes flush

Parameter	Symbol	Unit	Value
Darcy flux*	q	m/s	1×10^{-11}
Effective porosity	θ_{eff}	-	0.01
Contaminant velocity	v	m/s	1×10^{-9}
Average pit distance (Goose)	d	m	600
Time to flush for 1 pore volume	t	years	19 000
Time to flush for 3 pore volumes	T	years	57 000

* The value of darcy flux based on the FEFLOW model.

 SNC • LAVALIN	TECHNICAL NOTE Hydrogeological modelling for in-pit tailings deposition		Prepared by: E. Millet, G. Comeau Reviewed by: C. Belanger, H. Sangam	
			Rev.	Date
	SNC No. 651196-3000-4WER-0001 AEM No. 6118-E-132-001-TCR-003		A00	August 16 th , 2018
				Page 46

Long-term upward release of contaminants from the tailings to the supernatant was not considered since tailings consolidation at post-closure continues at an insignificant rate (SLI, 2018b). Most upward release will occur during the deposition phase as the tailings rapidly consolidate.

After the tailings deposition, the reclaim water from the pit lake will be treated during closure period and before breaching the Goose Dike. Based on the Pit Lake Stratification Modelling study (SLI 2018), the contaminant input from the tailings in the pit lake will be negligible over time.

4.1.3 Plume behavior

Chloride and arsenic will have a different behavior in the groundwater. Nevertheless, their migration is primarily controlled by the advective transport. Therefore, to understand the migration of contaminants, it is essential to understand the hydraulics of the aquifer first (Ravenscroft, 2009). In that sense, contaminant travel times will be directly correlated to the groundwater context: if the hydraulic gradient and the hydraulic conductivity are low, the migration rate will be slow and thus, the time for the contaminant to reach the potential receptors at lake level will be relatively high.

Chloride plume behavior

As mentioned in 4.1.1, chloride has been shown to be a nonreactive solute, meaning that it will behave like water. Thus, the dynamic transport of the chloride plume will be ensured by three (3) physical processes:


- > **Advection** is the transport of dissolved mass along the bulk flow direction, meaning that advection is the translation of a solute with the flow velocity. This is the principal mode of mass transport in most cases;
- > **Dispersion** causes spreading of the solute plume. Mechanical dispersion reflects the fact that not all dissolved mass in the porous medium travels at the average water flow velocity. Some paths are faster, some slower, some longer, some shorter;
- > **Diffusion** is the net movement of a dissolved mass from high concentrations to low concentrations, due to a concentration gradient alone, and occurs with or without groundwater flow.

Arsenic plume behavior

The groundwater velocity is the effective upper limit for the migration rate of arsenic (Ravenscroft, 2009). Besides this physical process, transport of arsenic in the groundwater is also affected by several chemical processes. One of the main processes is adsorption. The transport of dissolved chemicals and adsorption are closely related in that adsorption slows down the rate of transport of a chemical compared with the water flow rate (Appelo and Postma, 1993). Studies indicate that the concentrations of dissolved As(V) and As(III) are controlled by adsorption on iron and aluminum oxides and clays. The degree of attenuation depends largely on the contrast between pH and redox conditions of the plume and the receiving water (Ravenscroft, 2009).

The adsorption of As(V) is high and independent of pH at acidic pH values, and decreases with increasing pH in the range of 7 to 9 (EPA, 2004). Arsenic(V) adsorption will be lower in soils with high phosphate concentrations because of anion competition. Iron-reducing bacteria may cause arsenic mobilization from soils as a consequence of reductive dissolution of iron oxyhydroxide adsorbents. Sulfate reducing bacteria, in addition, may promote arsenic reduction by producing hydrogen sulfide (EPA, 2004).

Typical evolution of contaminant concentrations in the groundwater

 SNC • LAVALIN	TECHNICAL NOTE		Prepared by: E. Millet, G. Comeau Reviewed by: C. Belanger, H. Sangam		
	Hydrogeological modelling for in-pit tailings deposition		Rev.	Date	Page
	SNC No. 651196-3000-4WER-0001 AEM No. 6118-E-132-001-TCR-003		A00	August 16 th , 2018	47

Advection, dispersion, diffusion and adsorption act as attenuation processes since they tend to reduce concentrations of the plume. Figure 23a shows general impacts of various attenuation processes, and the overall bulk rates change as a result (i.e., the more processes present at a given site, the higher the bulk attenuation rate). Figure 23b could represent a typical contaminant concentration evolution at a fixed location like East Dike. Note that source decay and biodegradation are also attenuation processes but they were not considered in the present study.

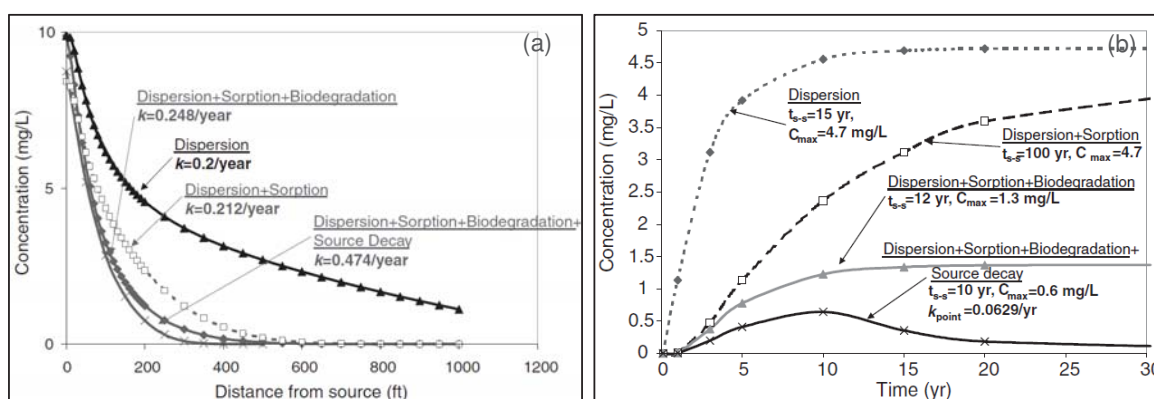


Figure 23 : Typical evolution of concentrations under various attenuation processes (a) along the plume and (b) at a fixed location downgradient (EPA, 2002)

4.2 Transport parameters


Transport parameters influence concentration and velocity of the contaminants in the groundwater. Effective porosities were based on field data and literature values, whereas other parameters (dispersivity, diffusion coefficients and K_d) were only based on literature values.

Effective porosity

Effective porosity θ_{eff} (unitless) is defined as the percentage of interconnected pore space. It represents the fraction of pore space that contributes to fluid flow and solute transport through the bedrock or sediments.

Contaminant transport is affected by effective porosity and thus particular attention was applied to values for bedrock as most of contaminant transport will occur at these depths. To do so, available televiwer surveys from the 2017 hydrogeological field investigation as well as from former geotechnical investigations were interpreted to estimate the total porosity of the bedrock. For the bedrock, effective porosity was assumed equal to the total porosity. Most of the televiwer data were gathered along the expected migration flow paths from the pits to receptors (lakes) and thus, reinforcing the applicability of these data for the targeted potential seepage zones.

Televiwer survey interpretations can provide structure types (close joints, slightly open joints, open joints) and the open joint apertures, if greater than the detection limit of the equipment (1.3 mm). For each identified slightly open joint, half the detection limit of the joint aperture (0.065 mm) was also considered in the porosity calculation. Open joint apertures and slightly open joint apertures were then summed to estimate the total porosity over 20 m thick

 SNC • LAVALIN	TECHNICAL NOTE Hydrogeological modelling for in-pit tailings deposition	Prepared by: E. Millet, G. Comeau Reviewed by: C.Belanger, H.Sangam		
		Rev.	Date	Page
	SNC No. 651196-3000-4WER-0001 AEM No. 6118-E-132-001-TCR-003	A00	August 16 th , 2018	48

bedrock sections. The result of these bedrock porosity estimates from 9 televiewer surveys is available at Figure 24.

Televiewer surveys and the related porosity estimates are limited to the first 200 m of bedrock (120 masl to -80 masl). The geometric mean curve (in red) gives a good approximation of the decreasing porosity with depth. Based on these televiewer observations, average bedrock porosity ranges from 0.004 to 0.0002 from the surface to about 100 m depth, where it is assumed to be constant. This porosity relation with depth was considered in the 3D model for transport simulations and the retained values for bedrock are available in Table 8. As a comparison, Domenico and Schwartz (1990) give effective porosity values for fractured crystalline rocks that are less than 0.0001. Guimera and Carrera (2000) also provide such low values of effective porosity for bedrock. Higher porosities have been found at Central Dike location (700-P1) and at greater depths at East flat (IPD-17-01). These higher porosities have been applied to Second Portage Lake Fault and Bay Fault. It is important to note that higher the effective porosities, the lower the plume migrate rate.

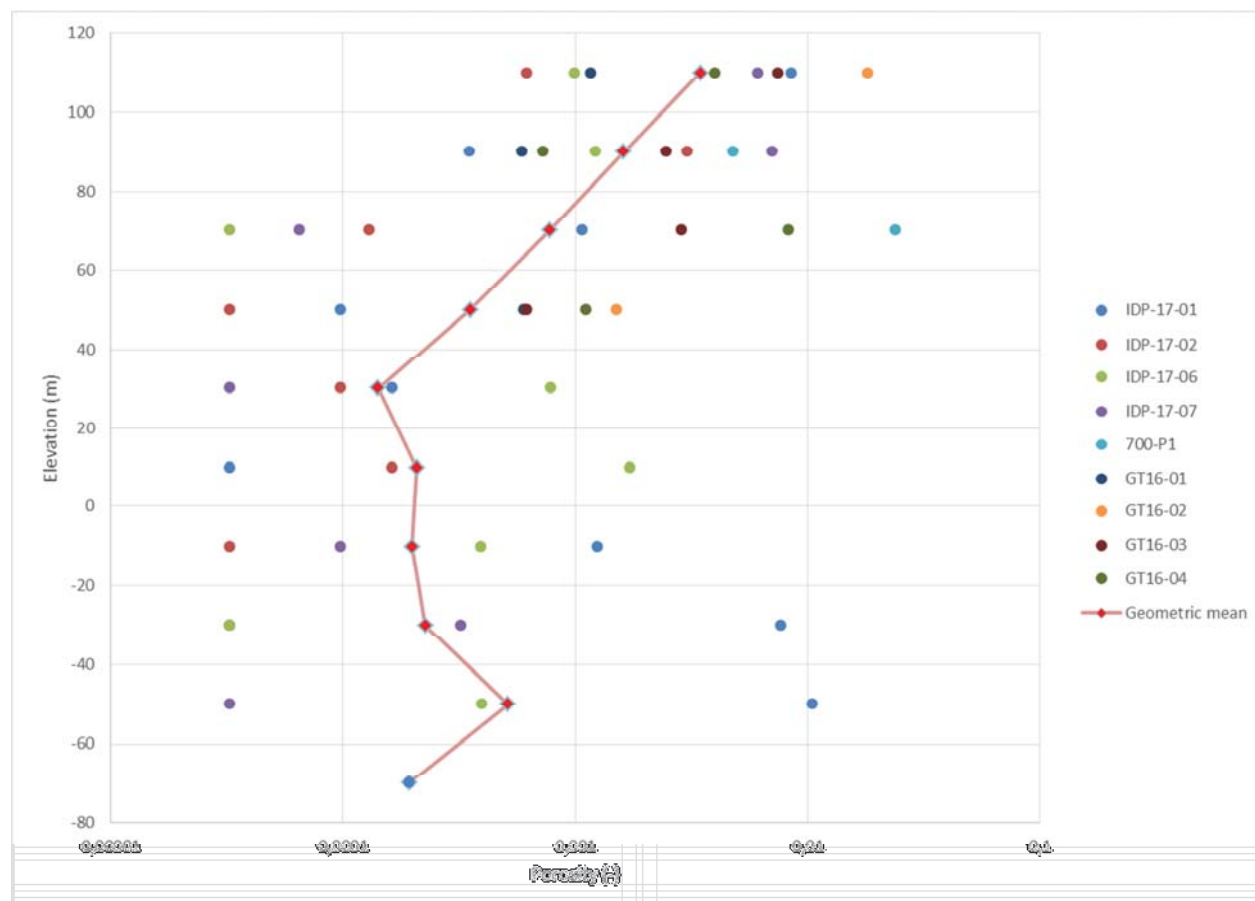



Figure 24 : Bedrock porosity by 20 m thick layer according to televiewer surveys

 SNC • LAVALIN	TECHNICAL NOTE		Prepared by: E. Millet, G. Comeau Reviewed by: C.Belanger, H.Sangam		
	Hydrogeological modelling for in-pit tailings deposition		Rev.	Date	Page
	SNC No. 651196-3000-4WER-0001 AEM No. 6118-E-132-001-TCR-003		A00	August 16 th , 2018	49

In-pit tailings effective porosity has been determined from the available laboratory tests (Golder, 2017) and based on a 1D consolidation model of the in-pit tailings deposits (SLI, 2018b).

According to the SLI (2018b), average solid content of tailings deposits in Goose Pit, Pit A and Pit E range from 78.3% to 79.3% at the end of deposition, meaning that the water content (or total porosity) will range from 26.1% to 27.6%. This also corresponds to a gravimetric water content (effective porosity) of 27%, resulting from the soil-water characteristic curve, performed in the laboratory by Golder (2017) on Amaruq tailings. After 40 years following the end of IPD, the average solids content would only increase by less than 1% and thus, would decrease the water content (total porosity) by the same magnitude. However, lower effective porosity was attributed to tailings because laboratory tests often overestimate this parameter by up to a factor of 10. Attributing lower effective porosity will accelerate contaminant migration.

Table 8 : Effective porosity used for transport simulations


Hydrostratigraphic unit	Layer	Effective Porosity used in the model (-)	Source
Bedrock	5 to 11	0.004	Televiewer analysis
Bedrock	12 to 17	0.0009	Televiewer analysis
Bedrock	18 to 50	0.0002	Televiewer analysis
Till deposit	1 to 4	0.17	Johnson (1967)
All faults	4 to 50	0.02	Max value from televiewer survey (IPD-17-01)
Portage waste rock	1 to 21	0.30	Arbitrary set value
TSF North Cell & South Cell tailings	1 to 3	0.027	Johnson (1967) for fine sand (0.23) and silt (0.08)
In-pit tailings	4 to 32 (for pit E)		Golder (2017) lab test SLI (2018b) Consolidation Memo

Adsorption (only for arsenic)

When solutes flow through a porous medium, they can interact with the solid phase. Adsorption is the process in which molecules present in the fluid adhere spontaneously to a solid surface. The result is a process called retardation that slows the transport of a solute through a porous medium.

Adsorption is the most important process that retards arsenic migration, and the most important sorbents are iron oxides (Ravenscroft, 2009). The way that adsorption retards the transport of arsenic can be expressed in a simplified way (for the case of a linear adsorption isotherm with a constant retardation factor) by the partition (distribution) coefficient K_d (L/kg) which describes its partitioning between the solid and liquid phases (Fetter, 1999):

$$K_d = \frac{s}{C}$$

 SNC • LAVALIN	TECHNICAL NOTE		Prepared by: E. Millet, G. Comeau Reviewed by: C. Belanger, H. Sangam		
	Hydrogeological modelling for in-pit tailings deposition		Rev.	Date	Page
	SNC No. 651196-3000-4WER-0001 AEM No. 6118-E-132-001-TCR-003		A00	August 16 th , 2018	50

where “s” is the concentration adsorbed to the soil (µg/kg) and “C” is the concentration dissolved in water (ppb), (Langmuir, 1997). This formula is a simplified relation because adsorption processes for arsenic are non-linear generally and thus the value of K_d varies with concentration (Nair and Pandey, 2013). Nevertheless, it gives a useful appreciation of how adsorption impacts contaminant concentrations.

In order to understand how K_d can affect contaminant concentrations in groundwater, we can introduce the retardation factor. The retardation factor R (unitless) describes the extent to which the migration of dissolved contaminants can be slowed down by adsorption to the aquifer matrix. The degree of retardation depends on both aquifer and contaminant chemical properties. R is the ratio of the groundwater seepage velocity (v_w) to the average velocity of a migrating contaminant (v_{As}). The retardation factor relates to the K_d by the following formula (Freeze and Cherry, 1979):

$$R = 1 + \frac{\rho_b}{\theta} * K_d$$

with, ρ_b is the dry bulk density (g/cm³), K_d is the partition coefficient (L/kg) and θ is the effective porosity.

Hence, the velocity of the contaminant can be expressed as:

$$v_c = \frac{v_w}{R}$$

where v_c is the velocity of the contaminant (m/s) and v_w is the velocity of water (m/s).

For chloride, K_d is equal to 0 L/kg, meaning there is no retardation of chloride in the groundwater. In contrast, the K_d value for arsenic (29 L/kg at pH 6.8 according to EPA, 1996) indicates that it will move slower in water than the chloride because of adsorption.

Typical K_d values and calculated retardation factors for identified chemical parameters of the reclaim water are available at Table A.4, Appendix A.

Dispersivity

Gelhar and Axness (1983) consider hydrodynamic dispersion D as an expression of uncertainty due to local-scale heterogeneity. Dispersion principally depends on the average linear velocity (scale dependent) times a property of the medium, called dispersivity α (Domenico and Schwartz, 1990), which can be expressed as:


$$D = \alpha * v + D^*$$

where α is the dispersivity (m), v is the average linear velocity (m/s), and D^* the diffusion coefficient m²/s.

The dispersivity acting parallel to the principal flow direction is called longitudinal dispersivity (α_L) and dispersivity in the perpendicular direction is called transverse dispersivity (α_T). Dispersivity values are particularly important with regards to contamination issues because dispersion spreads the plume by attenuating concentration gradients (Adams and Gelhar, 1992). Values of longitudinal and transverse dispersivity used the model (Table 9) were based on the model dimensions as proposed by Gelhar (1986).

Diffusion

Diffusion D^* (m²/s) is caused by random molecular motions due to the thermal kinetic energy of the solute. It describes the spread of the dissolved contaminants through random motion from regions of higher concentration to regions of lower concentration. In most hydrogeological models, diffusion is often neglected because it is typically not as large as mechanical dispersion. Since the Meadowbank site post-closure conditions present very low

 SNC • LAVALIN	TECHNICAL NOTE		Prepared by: E. Millet, G. Comeau Reviewed by: C. Belanger, H. Sangam		
	Hydrogeological modelling for in-pit tailings deposition		Rev.	Date	Page
	SNC No. 651196-3000-4WER-0001 AEM No. 6118-E-132-001-TCR-003		A00	August 16 th , 2018	51

gradients (hydraulic gradient at Goose Pit is less than 0.00005 m/m), however, the diffusion process was considered (Table 9).


Table 9 : Summary of transport parameters used for numerical simulations

Parameter	Symbol	Unit	Base case value	Source
Longitudinal dispersivity	α_L	m	15	Gelhar et al., 1992
Transverse dispersivity	α_T	m	1.5	Gelhar et al., 1992
Effective porosity	θ_{eff}	-	$0.0001 < \theta_{eff} < 0.3$	Televiewer analysis & literature (see Table 8 for more details)
Partition coefficient (As)	K_d	L/kg	29**	EPA, 1996
Partition coefficient (Cl)	K_d	L/kg	0**	EPA, 1996
Molecular diffusion (As)	D	cm ² /s	1E-05	Takahashi et al., 2011; Tanaka et al., 2013
Molecular diffusion (Cl)	D	cm ² /s	1E-05	Barone et al., 1992
Rock bulk density	ρ	g/cm ³	2.7	Golder, 2007 (Pit slope design criteria for the Portage and Goose island deposits – table 6.11)

** K_d values at pH 6.8. With a bulk density of 2.7 g/cm³ and an effective porosity of 0.0002, resulting Retardation factors (R) are 1 and 391 501, for chloride and arsenic, respectively.

4.3 Simulation results for chloride and arsenic

In order to assess a worst case scenario, transport simulations were performed post-closure, when all pits are filled with tailings (at a maximum elevation of 125.6 masl) and after maximum permafrost degradation after 100 years, as determined by the thermal assessment (SLI, 2018c). As mentioned previously, the contaminant source is located in the pore water of the in-pit tailings with a constant specific concentration for each pit, as based on the in-pit water quality assessment at closure (SLI, 2018a). The source concentration remained constant from the beginning to the end of the simulation as set in the conceptual model. Chloride and arsenic simulations were completed separately. Since flow velocities appeared to be very slow in the model, simulations were run for 10,000 years to be able to capture contaminant plume behavior on a long spatial scale. For both chloride and arsenic, the model showed that the earliest contaminant breakthrough was located at East Dike. An artificial observation well (W_{ED}) was introduced into the model at East Dike on the plume flow path to follow contaminant concentrations with time. This well was fixed over the entire thickness of the model in order to track contaminant arrival times at Second Portage Lake. Later, this observation well was also used in the sensitivity analysis to compare the contaminant arrival times for different parameter sets.

 SNC • LAVALIN	TECHNICAL NOTE		Prepared by: E. Millet, G. Comeau Reviewed by: C.Belanger, H.Sangam		
	Hydrogeological modelling for in-pit tailings deposition		Rev.	Date	Page
	SNC No. 651196-3000-4WER-0001 AEM No. 6118-E-132-001-TCR-003		A00	August 16 th , 2018	52

It is important to note that the following analysis gives forecast simulations for which no calibration was possible since no chemical concentration data were available, at closure and without pumping.

The following assumptions have been made for this post-closure modelling:


- > All pits (Goose Pit, Portage Pit A and Portage Pit E) are filled with tailings to an elevation of 125.6 masl;
- > Maximum permafrost degradation is based on the thermal assessment (SLI, 2018c)
- > North Cell TSF, South Cell TSF and the underlying till are frozen over their entire thickness to represent the thermal closure scenario, as modelled by OCK (2015) North Cell TSF Closure Design Report;
- > No further pumping occurs at Central Dike D/S Pond and East Dike pumping wells;
- > Goose dike has been breached;
- > Water cover has been treated after deposition (thus does not impact the groundwater modelling).

4.3.1 Chloride

Long-term patterns of the chloride plumes

After 10,000 years, simulation results showed three (3) plumes spreading from each pit towards Second Portage Lake, and then, reaching the outflow limit of the model, following the natural gradient (Figure 25a). Plumes coming from Goose Pit and Portage Pit E show practically the same behavior: the contaminant first migrates downwards with the local gradient (Figure 25b); then, it sinks below the permafrost toward the eastern outflow boundary of the model. After 10,000 years, higher concentrations are observed in the groundwater under Pit E because the source concentration at Pit E was the highest (141 mg/L versus 115 and 22 mg/L for Pit A and Goose Pit, respectively) as predicted by the in-pit water quality assessment at closure (SLI, 2018a).

For Pit A, the migration appears to be faster because the plume will travel more directly to the Second Portage Lake. Figure 25a shows that the migration path follows the Second Portage Fault plane. Since the direction of the gradient in Second Portage Lake arm is mostly horizontal, the spreading of the Pit A plume is also limited with depth (Figure 25b and Figure 28).

 SNC • LAVALIN	TECHNICAL NOTE		Prepared by: E. Millet, G. Comeau		
	Hydrogeological modelling for in-pit tailings deposition		Reviewed by: C.Belanger, H.Sangam		
	SNC No. 651196-3000-4WER-0001 AEM No. 6118-E-132-001-TCR-003		Rev.	Date	Page
			A00	August 16 th , 2018	53

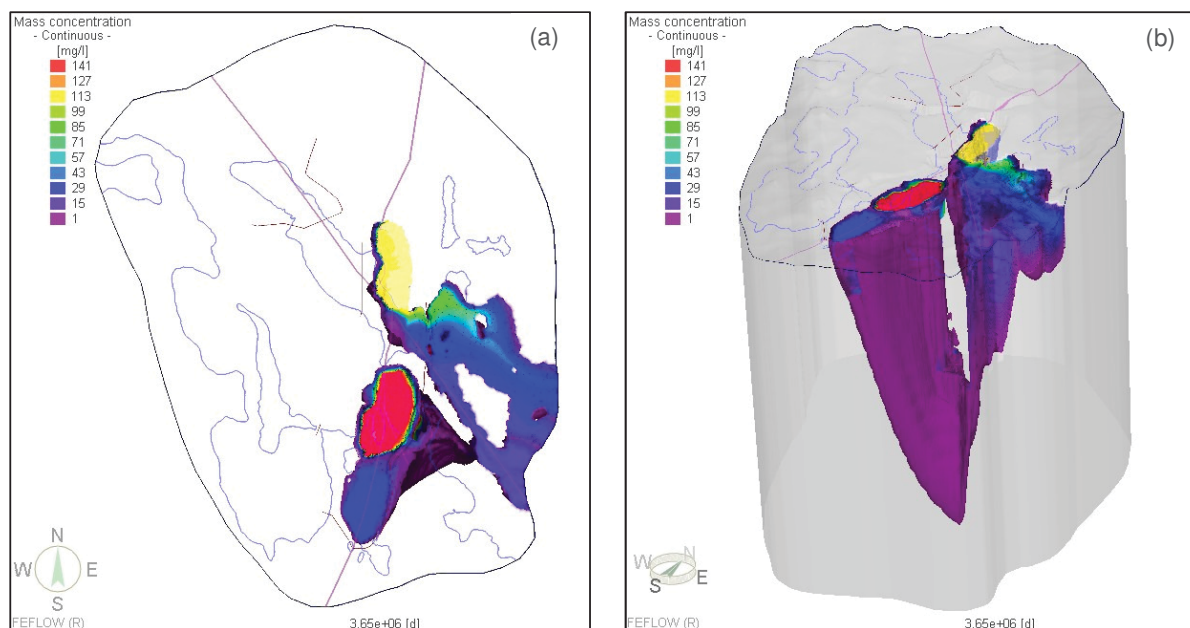



Figure 25 : Long-term patterns of chloride plumes after 10,000 years: (a) plan view and (b) 3D view from south-east with a 1 mg/L isocontour

First time arrival of Pit A chloride plume

A model observation well (W_{ED}) was set near East Dike (Figure 26) and a few observation points were introduced from the top to the bottom of the model. Concentration evolution with time at these observation points is shown in Figure 27. Each curve represents the chloride concentration for a different elevation in the model. Concentrations vary differently according to their elevation, reflecting the spreading of the plume in the vertical direction. At an early stage, we can see that concentrations were higher at depth (around -4 masl, green curve R-27-4), than in the upper part of the model. Indeed, the effective porosity is very low at this elevation (0.0002) compared to the overlying effective porosity of Central Dump (0.30). The contaminant will hence move faster under Central Dump, and will reach East Dike sooner. A section of the chloride plume from Pit A to Second Portage Lake, after 1000 years is shown on Figure 28.

 SNC • LAVALIN	TECHNICAL NOTE Hydrogeological modelling for in-pit tailings deposition	Prepared by: E. Millet, G. Comeau Reviewed by: C.Belanger, H.Sangam		
		Rev.	Date	Page
	SNC No. 651196-3000-4WER-0001 AEM No. 6118-E-132-001-TCR-003	A00	August 16 th , 2018	54

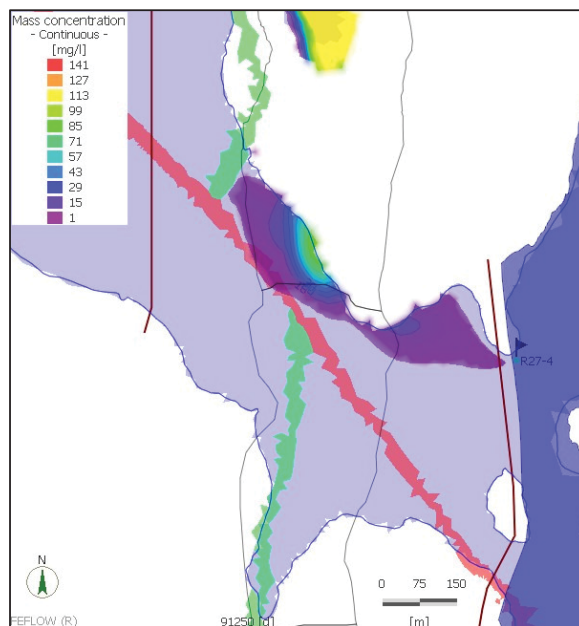



Figure 26 : Plume distribution on first breakthrough of the 1 mg/L chloride isocontour at East Dike after 255 years

Figure 27 allows concluding that:

- > Chloride at East Dike will never exceed the CCME criteria of 120 mg/L (Figure 27a), because the initial concentration of the Pit A source is 115 mg/L. The maximum concentration to reach East Dike will be around 85 mg/L which is less than the Pit A source initial concentration (Figure 27a). Indeed, dispersion will tend to spread the plume which will decrease maximum concentrations;
- > Breakthrough point of 50% of the Pit A plume chloride concentration, corresponding to 40 mg/L, will reach Second Portage Lake after 1100 years (Figure 27a);
- > First appearance of chloride will reach Second Portage Lake after 255 years with a concentration of 1 mg/L (Figure 27b). This concentration was chosen as low as possible to be able to be considered as the first appearance of the contaminant at the observation point.

 SNC • LAVALIN	TECHNICAL NOTE Hydrogeological modelling for in-pit tailings deposition	Prepared by: E. Millet, G. Comeau Reviewed by: C.Belanger, H.Sangam		
		Rev.	Date	Page
	SNC No. 651196-3000-4WER-0001 AEM No. 6118-E-132-001-TCR-003	A00	August 16 th , 2018	55

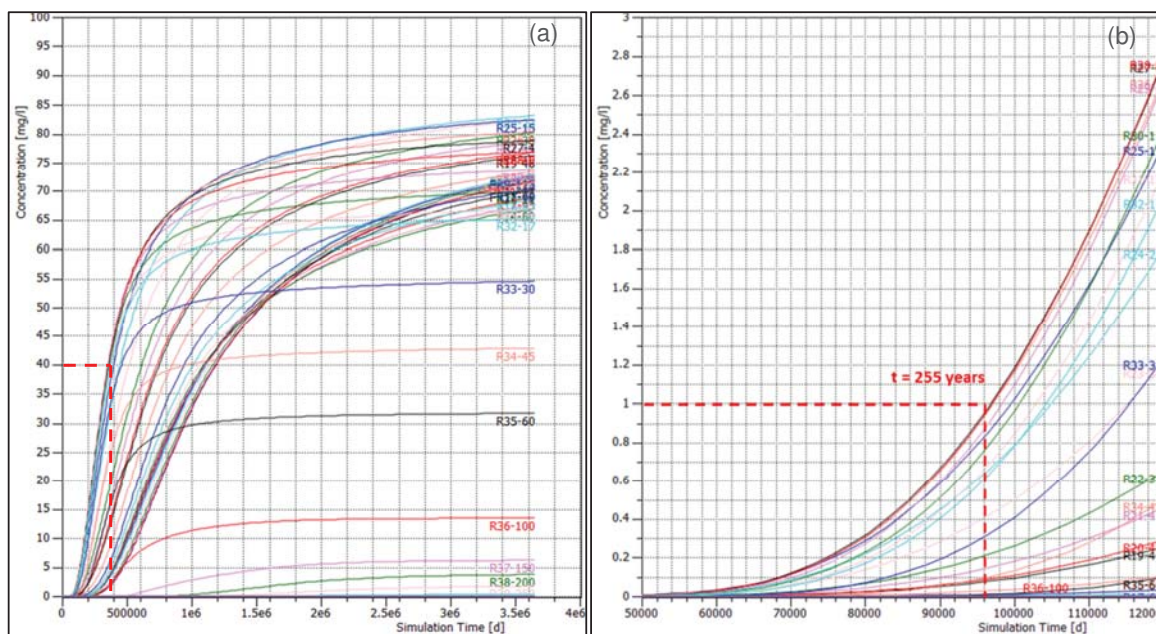



Figure 27 : Simulated evolution of chloride concentrations with time at W_{ED}; (b) is a zoomed-in view of (a)

 SNC • LAVALIN	TECHNICAL NOTE Hydrogeological modelling for in-pit tailings deposition	Prepared by: E. Millet, G. Comeau Reviewed by: C.Belanger, H.Sangam		
		Rev.	Date	Page
	SNC No. 651196-3000-4WER-0001 AEM No. 6118-E-132-001-TCR-003	A00	August 16 th , 2018	56

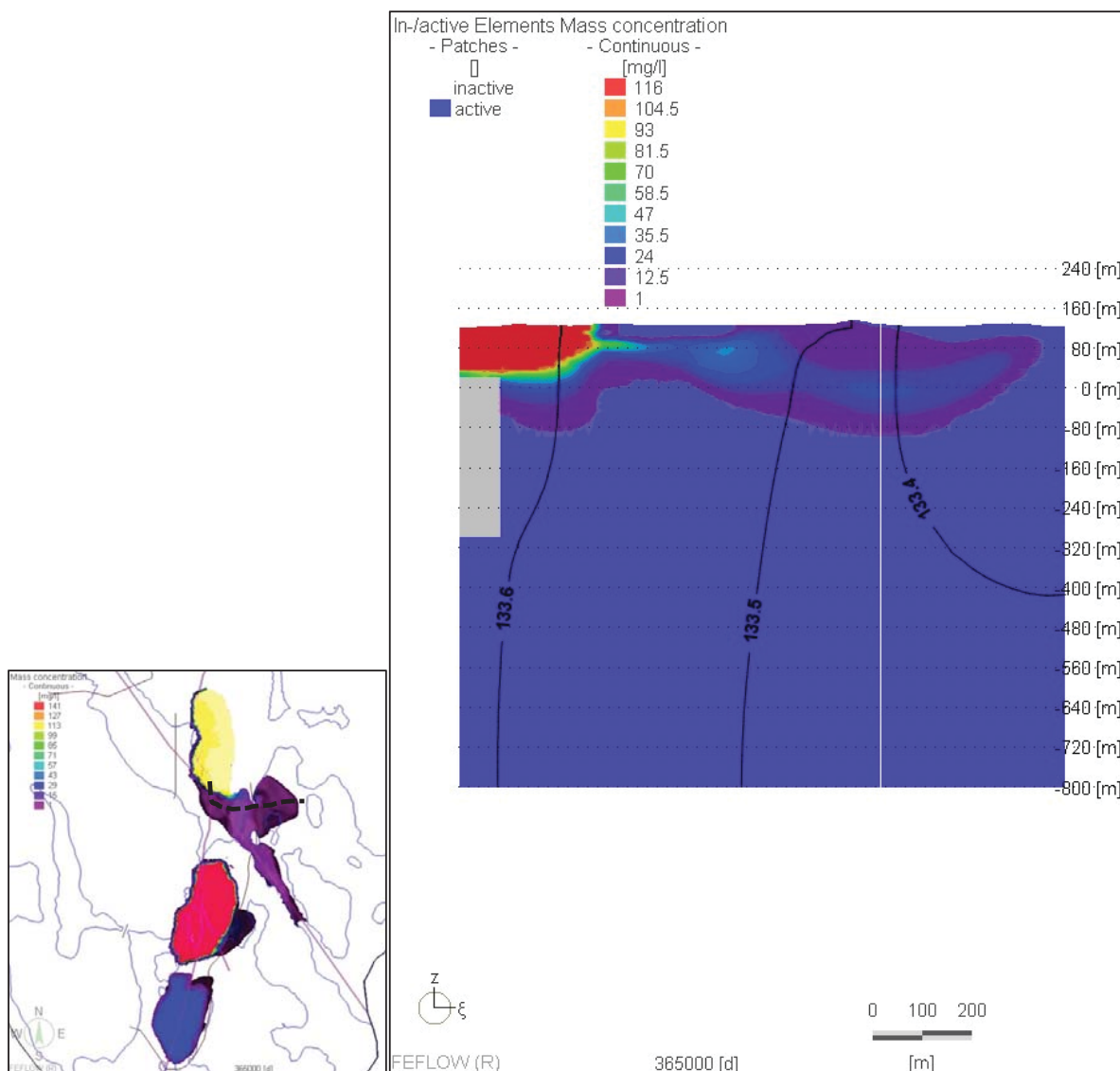



Figure 28 : Vertical section of predicted chloride concentrations from Pit A, 1000 years after in-pit deposition

 SNC • LAVALIN	TECHNICAL NOTE Hydrogeological modelling for in-pit tailings deposition	Prepared by: E. Millet, G. Comeau Reviewed by: C. Belanger, H. Sangam		
		Rev.	Date	Page
	SNC No. 651196-3000-4WER-0001 AEM No. 6118-E-132-001-TCR-003	A00	August 16 th , 2018	57

Portage Pit E and Goose Pit plumes

Contaminant migration from Portage Pit E and Goose Pit is occurring vertically, underneath the pits and surrounds the base of the permafrost. Figure 25b shows both plume direction from Pit E and Goose Pit, 1000 years after in-pit deposition. A vertical section of the plume from Pit E and Goose Pit is also provided on Figure 30 and Figure 31, respectively. For both Portage Pit A and Goose Pit, general observations are as followed:

- > At $t = 1000$ years, the plume from Pit E has not reached Second Portage Lake (Figure 29b) because the lateral migration that is shown occurs at depth (-300 masl), below the permafrost;
- > Vertical migration represents the main pathway from Pit E and Goose Pit to the outflow boundary of the model;
- > Nevertheless, after 10 000 years, a small part of the Goose Pit and Portage Pit E plumes will reach Third Portage Lake by lateral migration, but concentrations will not exceed 50 mg/L;
- > After 10 000 years, chloride from Portage Pit E and Goose Pit haven't reached the outflow boundary of the model because of the long migration time under the permafrost;
- > Over a 10 000-year simulation, concentrations at Second and Third Portage Lake remain below the CCME criteria of 120 mg/L;
- > Although the permafrost is thawed in the northern upper part of Pit E, the model does not suggest a contaminant migration towards Central Dump.

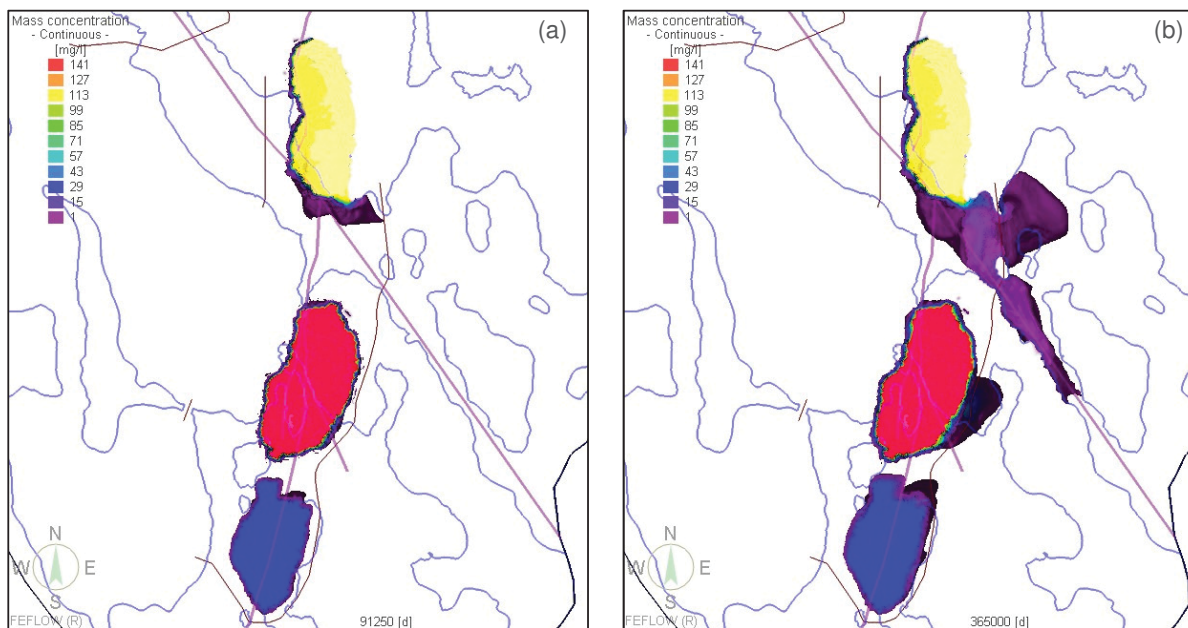


Figure 29 : Simulated evolution of chloride migration from Pit E and Goose Pit after (a) 250 years and (b) 1000 years